DEVELOPMENT OF A MEMBRANE PHOTOBIOREACTOR FOR THE STUDY OF MICROCYSTIN PRODUCTION BY CYANOBACTERIA

Final Report to the Water Research Commission

by

W D Leukes, *J Strong, and *T C Downing

Department of Biochemistry, Microbiology & Biotechnology
Rhodes University
Grahamstown

*Department of Microbiology
University of Port Elizabeth
Port Elizabeth

WRC Report No 1103/1/03

ISBN No 1-77005-076-0

OCTOBER 2003

Disclaimer

This report emanates from a project financed by the Water Research Commission (WRC) and is approved for publication. Approval does not signify that the contents necessarily reflect the views and policies of the WRC or the members of the project steering committee, nor does mention of trade names or commercial products constitute endorsement or recommendation for use.

ACKNOWLEDGEMENTS

Water Research Commission and National Research Foundation for financial assistance.

Rhodes University Electron Microscopy Unit for cutting sections and use of their facilities.

Dr. E.P. Jacobs of the University of Stellenbosch and Prof. V. Linkov of the Western Cape for membranes.

Dr. Gerhard Offringa for his assistance in management of the project.

EXECUTIVE SUMMARY

Introduction

Cyanobacterial blooms are a commonly occurring phenomenon in water bodies due to increasing nutrient levels from industrial effluent and agricultural soil leachates. This increases the potential of blooms that produce toxic secondary metabolites, which are harmful to human and animal consumers. These toxins include neurotoxins as well as hepatotoxins such as microcystins. It is important to develop suitable laboratory tools to study biofilms of Cyanobacteria, so that a better understanding can be obtained of the environmental factors that affect their occurrence and functioning. In addition, microcystin standards for analytical use are extremely expensive, difficult to obtain and there is a growing demand for standards of the more common variants. This project was therefore undertaken to develop a membrane photo-bioreactor as a tool for the study of algal biofilms as well as a potential tool for production of toxins.

By immobilizing bacteria on membranes it was found to be possible to manipulate their environment such that a particular nutrient concentration can be achieved at extra-capillary membrane surfaces, allowing for a nutrient gradient that decreases from the interior to the exterior of the biofilm. With *Microcystis aeruginosa* PCC7806 secondary metabolite (microcystin LR and Asp-microcystin LR) production was obtained, which appeared to be modulated by temperature, nutrient ratios and concentrations and light intensities. Synthetic membrane modules would allow for fine-tuning of such ratio's and concentrations within the biofilm thus, theoretically, allowing analysis and fine control of toxin production in biofilms.

Methodology

The first stage of the project involved acquisition of relevant information of the factors that would affect toxin production, bacterial immobilization and methods of toxin extraction from the cyanobacterial biofilm.

The second stage of the project involved development of a suitable membrane module and a method to immobilize the bacteria. Externally skinless polyethersulfone capillary membranes were evaluated in this study. Adsorption, pressure and cell slurry immobilization techniques were tested for the establishment of a biofilm on the

membranes. Each module and immobilization technique had inherent advantages and disadvantages. The variability with bacterial adherence was also investigated.

The third stage of the project was to assess toxin production in the biofilm. Toxin production was measured as a function of time, biofilm thickness, nitrate concentration and light intensity. Toxin production was then established with a 4 X 2 factorial experiment using time, light intensity, nitrate concentration and biofilm thickness as primary factors. An immunolabeling technique was developed in order to establish where in the biofilm toxin production was greatest.

Results

The externally skinless polyethersulfone membranes showed good potential for biofilm establishment. Of the techniques tested for immobilization the best result was achieved with pressure filtration inoculation. The cell slurry adsorption technique also showed promise but had the disadvantage of contaminants being easily introduced. Adsorption was not a feasible method for rapid biofilm development.

Buoyant cells in a rapid state of division, having less developed cell walls, did not adhere well to the membranes. Non-buoyant cells with a well-developed extracellular polysaccharide layer adhered to one another and the membranes well.

Toxin production appeared to be rapid with the immobilized cells, but the yields were low. According to the experiments a high nitrate concentration in the lumen and a moderate light intensity were optimal for toxin production at 25^{o}C. Toxin was produced optimally above the pore openings, where there was a higher light and nutrient concentration. The production of toxin occurred in veins, due to quicker diffusion of nutrients through channels formed during the immobilization procedure.

Conclusion

Although toxin production is rapid using this system, the biomass development and total toxin produced is low at this stage of development of the project. Further optimisation needs to be done once a better understanding of the physiology of the biofilm has been obtained. The cells also have to pass through their most productive stage of toxin production before they immobilize well. Toxin production occurred in clusters around the

pore openings, where the nitrate concentration and light intensity was higher. Veins of microcystin production occurred in the biofilm as channels formed during immobilization allowed for nutrients to diffuse to the outer biofilm more rapidly than the lateral movement (parallel to the lumen) of nutrients. Thus considerable new information was obtained on the physiology of microcystin production using a membrane bioreactor as a research tool. However, as a tool for production of microcystin as analytical standards, further optimisation would be required, particularly with regard to product extraction.

TABLE OF CONTENTS

LIST OF FIGURES

LIST OF ABBREVIATIONS

ADDA	= 3-amino-9 methoxy-2, 6, 8-trimethyl-10-phenyldeca-4, 6-dienoic acid
APES	= 3 - amino - propyl – triethoxy - silane
Asp	= aspartinine
BG-11	= Chemically defined growth medium
BSA	= bovine serum albumin
CM	= capillary membrane
Dasp	= Asp having a methyl group replaced by hydrogen atom
DIG	= dioxygenin
DMSO	= dimethyl sulfoxide
ECS	= Extracapillary space
EDTA	= ethylene diamine tetra-acetic acid
EPS	= extracellular polysaccharide
ESCM	= externally skinless polyethersulfone capillary membrane
Fc	= Constant fragment
%G+C	= percentage guanine + cytosine
HF	= hollow fibre
HPLC	= high performance liquid chromatography
IgG	= immunoglobulin G
LD_{50}	= lethal dose that kills 50% of the subjects
M	= methionine
NBT/BCIP	= napthol-As-phosphate/diazonium salt
N:P	= nitrate:phosphate ratio
OD_{740}	= optical density at 740nm
OsO_4	= osmium tetroxide
LM	= light microscopy
PBS	= phosphate buffered saline
PBST	= PBS containing Triton X-100
PDA	= photodiode array
pNP	= para-nitrophenyl
pNPP	= para-nitrophenyl phoshate
PP	= protein phosphatase
PPI	= protein phosphatase inhibition
R	= arginine
SEM	= scanning electron microscopy
TEM	= transmission electron microscopy
Tris-HCl	= Tris hydrochloride
v	= volume
w	= weight
WS	= website
λ_{max}	= maximum absorption wavelength

CHAPTER 1

LITERATURE REVIEW

1.1 Introduction to the cyanobacteria and *Microcystis aeruginosa*

Natural toxins (poisons of plant, animal, fungal and bacterial origin) can affect a large number of humans or animals at a given time via contaminated food or drinking water. Algae and aquatic bacteria are two groups of microorganisms that include toxin-producing species that can detrimentally affect human and animal health. A particular group of bacteria known as the cyanobacteria (also referred to as blue-green algae) contain several toxin-producing strains (Skulberg *et al*., 1984).

The cyanobacteria are a class of pigmented prokaryotes containing about 150 genera and about 2000 species. They are the most diverse and widespread of the phototrophic prokaryotes. They differ in morphology, structure, and in their mode of response to environmental stimuli. Morphological differences include cell width, length, shape and production of heterocysts and akinetes, and their position in the trichomes. Cell constituents can include structures such as glycogen granules, lipid globules, cyanophycin granules, polyphosphate bodies as well as gas vesicles. The cyanobacteria have a photosynthetic apparatus similar in structure to the eukaryotic chloroplast, and are relatively larger than the average eubacteria, which led early taxonomists to classify them as algae (Falconer, 1993).

Cyanobacteria produce a large number of compounds with varying degrees of bioreactivity including micropeptins, cyanopeptolins, oscillapeptin, microviridin and aeruginosans, but only certain of the genera are known to produce toxic secondary metabolites. The toxins are divided into three basic groups, which are hepatotoxins, neurotoxins and lipopolysaccharide endotoxins. The hepatotoxins are microcystin and nodularin, while the neurotoxins include anatoxins and saxitoxins.

Microcystis aeruginosa belongs to the *Chroococales* order, has a general form of unicellular rods or cocci and forms non-filamentous aggregates. *M. aeruginosa* reproduces by binary fission or budding and does not form heterocysts. The *Chroococales* have a %G+C of 40-49 and are almost always non-motile, other than by vertical movement enabled by gas vesicles (Prescott *et al*., 1996). Bloom formation is common with *Microcystis aeruginosa*. It has been implicated in human health problems and has often been associated with the poisoning of animals throughout the world, including South Africa, Canada, USA, USSR, Australia, India,

Argentina and Japan. The toxic strains of the species produce one or more low molecular weight toxins, which have been designated as fast death factors and are shown to be a pentapeptide (known as nodularin) or a heptapeptide (microcystin) compound. (Frazier *et al*., 1984; Falconer, 1993; Rae, 1999 and van der Westhuizen and Eloff, 1985).

1.2 The Hepatotoxins

This is the largest group of the cyanobacterial toxins, currently consisting of 89 microcystins and nodularin (WS1). Microcystins and nodularin both have the unique amino acid known as the ADDA (3-amino-9 methoxy-2, 6, 8-trimethyl-10-phenyldeca-4, 6-dienoic acid) moiety, which gives the characteristic spectral peak at 238 nm. The microcystins are cyclic heptapeptides, with five of the amino acids common to all variants and two amino acids that are variable. The five common amino acids consist of three D-amino acids and two unusual amino acids (N-methyl dehydroalanine and ADDA), while the two variable amino acids in positions 2 and 4 are L-amino acids. The toxin's name is derived using abbreviations for the two variable amino acids e.g. microcystin LR: L = leucine and R = arginine. Other amino acids that are components of microcystins include: A = alanine, Y = tyrosine M = methionine and W = tryptamine. There are other minor variants such as Dasp microcystin LR, where a methyl group of the aspartamine has been replaced by a hydrogen atom (Gathercole and Thiel, 1987; Fastner *et al*., 1998). Microcystin has two ionizable carboxylic acid groups and one ionizable amine group has found to be stable over a pH range of 1-10 (de Maagd *et al*., 1999).

Microcystins and nodularin have been implicated in tumor promotion. Eukaryotic protein phosphatases 1 and 2A (designated as PP1 and PP2A) are inhibited by these toxins (Ash *et al*., 1995; van der Westhuizen and Eloff, 1985). Reversible protein phosphorylation is the major mechanism by which the body controls a variety of biological processes including metabolism, cell differentiation and proliferation and gene expression. During protein phosphorylation phosphate moieties are transferred from adenosine triphosphate molecules to the serine, threonine or tyrosine residues of proteins by protein kinases, and are hydrolyzed by protein phosphatases. The phosphorylation state of proteins controls their activity, switching them between active and inactive states. Serine-threonine phosphatases are divided into two main classes PP1 and PP2 (PP2 further subdivided in PP2A, PP2B and PP2C) based on susceptibility to endogenous inhibitors and substrate specificity. Both PP1 and PP2A contain a structurally related catalytic sub-unit that shares 50% amino acid identity. Much of the present knowledge of serine-threonine phosphatases has come from studies involving

their inhibition. Although some of the natural toxins are PP2A selective, there are none that are highly selective for PP1.

Although the general structure of microcystins and nodularin is not similar to okadaic acid, they do bind to the same receptors. Okadaic acid is a potent inhibitor of PP1and PP2A and a potent tumour promoter on mouse skin. The enzyme inhibition leads to the destruction of the cytoskeletal arrangement and the sinusoids (capillaries) of the liver cells. Research performed on protein phosphatase inhibition has indicated the nodularin to be more a more potent inhibitor than three microcystin variants (microcystin LR, YR and RR), while okadaic acid displays inhibition similar to microcystin YR and LR (Yoshizawa *et al.,* 1990).

Some of the symptoms displayed by animals suffering from hepatotoxicosis include necrosis of the liver, pallor, violent convulsions, vomiting, diarrhoea, weakness, photosensitivity and cold extremities. Symptoms displayed by humans include acute hepatitis, fever, pains in the muscles and joints, vomiting, skin rashes, diarrhoea and eye irritations. Death normally results from hypovolemic shock caused by the pooling of the blood in the hepatocytes (Rae *et al*., 1999; Gorham, 1964).

Lethal dosage values reported differ from animal to animal and the results recorded for oral toxicity were generally higher than those recorded for intraperitoneal injections. Factors such as age, sex, and amount of food in the gut may affect the toxicity, but there is no reliable extrapolation by which lethal dosage concentrations in laboratory animals can be applied to humans. In 1996 43 patients died in a Brazilian hospital from suspected microcystin LR poisoning introduced from the water used in the kidney dialysis. Tests to the water and filters in the dialysis equipment resulted positive for microcystin LR (Rae *et al.,* 1999).

The presence of D-amino acids in microcystins strongly suggests that toxin production in the *Microcystis* genus is mediated by a non-ribosomal mechanism. Bacitracin, a peptide that is structurally similar to toxic peptides produced by *Microcystis* strains, is synthesized non-ribosomally in *Bacillus* strains. Non-ribosomal peptide synthesis is achieved in prokaryotes and lower eukaryotes, by the thiotemplate function of large, modular enzyme complexes that are collectively known as peptide synthetases.

Non-ribosomal peptide synthesis is achieved in prokaryotes and lower eukaryotes by the thiotemplate function of large, modular, enzyme complexes that are collectively known as

peptide synthetases. The majority of these non-ribosomal peptides are classified as secondary metabolites. They rarely have any use in primary metabolism, growth or reproduction, but have evolved such that the microorganism does somehow benefit from their production. These secondary metabolites can function as antibiotics, cytostatics, immunosuppressants, enzyme inhibitors and other cellular effectors. Specific detection of the gene cluster for microcystin has been reported for both cultured and non-cultured samples. (Neilan *et al*, 1999)

1.3 Factors that influence cell growth and toxin production

The concentration of the microcystins and nodularin vary according a number of stimuli including temperature, light intensity and wavelength, pH, osmotic potential, as well as nutrient ratios and variation of their concentrations.

Environmental factors that are favourable to bloom formation include a water temperature of 15 to 30^{o}C, moderate to high light intensity, a pH of 6-9, moderate to high nutrient levels (such as phosphates, nitrates and ammonia) and adequate aeration.

Optimal bloom conditions are not necessarily optimal for toxin production. Data from a study relating environmental stimuli changes to toxin fluctuation at the Hartebeespoort Dam found a direct correlation between increased temperature and solar radiation with toxicity. It was difficult to relate nutrient concentrations to microcystin production with their data, as concentrations fluctuated substantially over the two-year period and data reflected growth of a mixed population. Dominant bacteria would not necessarily have been toxin - producing species (Wicks and Thiel, 1990).

1.3.1 Stage of growth

Optimal production of microcystin in closed batch systems occurs at late exponential growth phase (Watanabe *et al*., 1985). At stationary phase there is normally some deprivation factor, which results in the production of secondary metabolites. At a certain cell density to nutrient concentration the switch over to stationary growth phase commences, and just prior to the switchover is when the microcystin variants are at their highest concentration.

1.3.2 Temperature and growth rate:

Temperature has a pronounced effect on toxicity and growth. van der Westhuizen and Eloff (1985) found the best growth rate for *M. aeruginosa* to occur at 32^{o}C, while at 16^{o}C the growth rate was less by a factor of 5.5. The highest toxicity was achieved when grown at 20^{o}C, with a LD_{50} of 25.4 mg.kg^{-1} with mice injected intraperitoneally. Toxicity was markedly reduced when the growth temperatures exceeded 28^{o}C (56-140 mg.kg^{-1}) and was halved at 16^{o}C. Highest production of toxin occurred with a culture that had a 2.8 day doubling rate, which was slower than the highest achieved doubling rate of 1.24 days.

Winter samples in a study of the Hartebeespoort dam were found to have low levels of toxicity (minimum temperature recorded was 13^{o}C). This could have been due to the prevalence of a non-toxic strain, but was more likely attributed to low temperature.

1.3.3 Light intensity

Kaebernick *et al.* (2000) found mcyB RNA transcript concentrations for *Microcystis aeruginosa* PCC7806 to exhibit two significant increases with increasing light intensity. The first light intensity threshold occurred between dark and low light (16 µmol.photons.m^{-2}.sec^{-1}) and the second between medium (31 µmol.photons.m^{-2}.sec^{-1}) and high light (68 µmol.photons.m^{-2}.sec^{-1}). No further increases were found when the cells were exposed to a higher light intensity of 400 µmol.photons.m^{-2}.sec^{-1}.

van der Westhuizen and Eloff (1985) found toxicity to decrease at the lower and higher light intensities tested. An intermediate light intensity provided for optimal toxin production. The highest production occurred with the culture that had a doubling time of 2.2 days at 145 µmol.photons.m^{-2}.second^{-1}. Highest toxin production was not found to correlate with the highest growth rate, and *M. aeruginosa* adapted physiologically to increasing light intensity with an increase in gas vesicle production and altering its pigment composition. Toxicity and growth were found to be minimal at their lowest tested intensity of 21 µmol.photons.m^{-2}.second^{-1}.

Microcystis species grow very slowly in laboratory cultures, and appear to be most affected by light intensities when grown in conical flasks. Under higher light intensities blooms tend to shift in prevalence from cyanobacteria to green algae. Other features included diminished cell size, and loss of colony formation. Under lower intensities the *Microcystis* cells retain their original characteristics such as buoyancy, colony formation, and toxicity. A major

problem experienced with the study of cyanobacterial cultures in blooms was the infiltration of other bacteria (Rae *et al*., 1999).

Variation of light intensity in calm waters leads to the establishment of strata of cyanobacteria that vary in toxicity with depth. Reports conflict as to whether light intensity or temperature is the controlling factor for microcystin production. Results for many different strains of *M. aeruginosa* as well as some *Anabaena*, *Aphanizomenon* and one *Oscillatoria* species indicate that light is the controlling factor, but below certain temperatures toxin production is still minimal (Utkilen and Gjolme, 1992; Utkilen and Gjolme, 1995; Rapala *et al*., 1997 and van der Westhuizen and Eloff, 1985).

1.3.4 Nutrient ratios and concentration variation (Phosphates, nitrates and iron)

A case of microcystin toxicosis was reported in a mid November in Georgia in the USA. Three cattle died as a result of drinking from a pond that contained a dense bloom of cyanobacteria. This was uncommon as the usually cold early winter temperatures prevented blooms. The area surrounding the pond had been fertilized with a high nitrogen compound two weeks prior to the noted bloom, and heavy rains had occurred just after the fertilization (Frazier *et al*., 1998).

Some tests have found no variation in toxin production under nitrate and phosphate limiting conditions. Utkilen and Gjolme (1995) found that increasing the iron concentration increased the ratio of toxin to dry weight with *M. aeruginosa* CYA 228/1. Increasing the iron concentration also increased the amount of microcystin RR toxin to protein ratio slightly. The variation of the phosphate concentration to resulted in an increase in the ratio of microcystin RR to dry weight, a slight decrease in the microcystin RR to protein ratio and the microcystin RR to dry-weight-minus-carbohydrates ratio to be unaffected. An increase in nitrate concentration resulted in an increase in microcystin RR to dry weight and dry weight minus carbohydrates, while the microcystin RR to protein ratio remained constant.

Watanabe and Oishi (1985) found phosphate limited conditions to decrease the growth rate slightly and decrease the toxin concentration negligibly. However under nitrate limiting conditions the growth rate decreased slightly, but toxicity decreased substantially. Utkilen and Gjolme (1995) also found lowered nitrate concentrations to result in a decrease in toxicity. They were assaying for microcystin RR production by *M. aeruginosa* CYA 228/1.

Oh *et al.* (1999) found the specific growth rate of *M. aeruginosa* UTEX 2388 to be a function of cellular phosphate under phosphate limitation. They found the growth rate reduced under phosphate-limited conditions due to a low carbon fixation rate, but the microcystin content of cells was higher. Consequently the toxin per dry weight was found to increase under phosphate limited conditions, even though toxin production rate was found to be linearly proportional to growth rate.

Lee *et al.* (2000) investigated the effect of nitrate:phosphate N:P ratios (1, 5 ,16, 50 and 100) on toxin production by *M. aeruginosa* UTEX 2388. Under a phospate-fixed condition the toxin content of the cells changed with altering ratios. The highest toxin production occurred at a (N:P) ratio of 16 (2.748 mg toxin.g dry mass) after an incubation of 7 days.

Wicks and Thiel (1990) did not show any correlation between organic and inorganic nutrient concentrations and toxin production by *M. aeruginosa*. Their data showed toxin production to correlate better with environmental factors such as increased solar radiation and temperature. It should be noted that their data relates to the bacteria in a natural environment, and not under laboratory conditions.

1.3.5 Aeration

Wicks and Thiel (1990) found an aeration rate increase from 100 to 1000 $mL.min^{-1}$ more than doubled the toxicity of a culture (*M. aeruginosa* NRC-1) that was grown under otherwise optimum conditions. Vigorous aeration results in increased and more uniform exposure of the cyanobacteria to the radiation source. This effect would be more important as the cell density (and therefore shading) increases, especially near the stationary growth phase, where cell density is at its greatest.

1.3.6 Light wavelength

Not only does intensity of light have an effect secondary metabolite production, but also the light type. When *M. aeruginosa* was grown under an intensity of 20 $\mu mol.m^{-2}s^{-1}$ for white, green and red light higher toxin concentrations were prevalent for cells exposed to red and green light than for cells exposed to white light (Utkilen and Gjolme, 1992).

Kaebernick *et al.* (2000) found mcyB RNA transcript concentrations greater for *Microcystis aeruginosa* PCC7806 exposed to red light relative to exposure to blue light. Cells were

moved from low white light to red and blue light of the same intensities. Cells under red light exhibited an increase in transcript levels equivalent to exposure to a high light intensity.

1.3.7 pH

pH tests done over a range of 6.5 to 10.5 (by the controlled addition of carbon dioxide: $H_2O + CO_2 <=> H_2CO_{3(aq)} <=> H^+_{(aq)} + HCO_3^-{}_{(aq)} <=> H^+_{(aq)} + CO_3^{2-}{}_{(aq)}$) found maximum toxicity to occur at the upper and lower ends of the pH studied; which correlated to the slowest growth rate for the organisms. In the studies that were done at the Hartebeespoort Dam, where the pH ranged from 7.7 to 9.4, the toxicity was found to increase as the pH increased (Wicks and Thiel, 1990).

1.3.8 Growth medium salinity

Blackburn *et al*. (1996) found minimum and maximum salinities tested did not favour the growth of *Nodullaria spumigena*, an estuarine bacterium. Nodularin content increased to the highest level between logarithmic and stationary phase, but as the extreme salinities of the growth medium resulted in decreased toxin content (Blackburn *et al*., 1996).

1.4 Immobilization of fungi and cyanobacteria

Surface environments are protective and offer the attached microbe a nutritional advantage. Many aquatic bacteria are dependent on attachment for survival in oligotrophic environments where low nutrient concentrations would normally not allow for growth. Bacteria are normally attached when living under low nutrient conditions and pelagic when in nutrient rich conditions. Cells within the biofilm are attached to each other and the substrate via their glycocalyx. Metabolites produced during bacterial growth can lead to surface damage that can result in the loosening of the biofilm. Similarly nutrient deprivation at the base of the biofilm can lead to cell death and result in sloughing of the biofilm.

The first stage of the biofilm development involves the reversible adsorption of the cells onto the surface. The next stage of development involves the production of extracellular adhesive materials, which occur as either as a covalently bonded capsular polysaccharide layer, or as a slime polysaccharide layer that is loosely associated with the surfaces. Exopolysaccharides (EPS) can act as an adhesive agent, play a role in nitrogen fixation, allow for protection from desiccation (as it is highly hydrated), protozoan predation (phagocytocis), osmotic shock,

enzymatic attack and may play a role in the uptake of metal ions. Attachment via the EPS to plastics can take a few hours e.g. Teflon and polystyrene due to the hydrophobic nature of the surfaces. Some success has been had with attachment of bacteria to positively charged surfaces such as platinum; but for the negatively charged surfaces such as glass and mica the attachment potential is low (Barbosa and Alterthum, 1992; Brown and Lester, 1980 and Prescott *et al*., 1996).

Experiments done with the immobilization of aerobic fungal cells (*Aspergillus niger*) on a dual hollow fiber bioreactor for the continuous production of citric acid resulted in yields that were 15.8 to 27 times greater (using air and oxygen respectively) than that of shake flask fermentation. There was a significant improvement in final concentration, yield and volumetric productivity relative to batch fermentation (Chung and Chang, 1987).

The production of bioactive substances such as antibiotics by cyanobacteria is very promising, as they can be grown under autotrophic conditions, and their growth medium is cheaper than that of heterotrophic bacteria. Low inorganic nutrient concentrations of the media can limit the growth of contaminating microorganisms.

In the case of filamentous bacteria a variety are known to produce intracellular and extra-cellular metabolites with diverse biological activities. *Scytonema* TISTR 8208 has been immobilized on polyurethane strips (floating as well as anchored) in a glass column photobioreactor with the aim of antibiotic production. Free-floating polyurethane strips could only immobilize 70% of the total cells inoculated with, whereas the stationary polyurethane strips immobilized 97% of the inoculum. The culture was sparged with air containing 5% CO_2 for agitation and a carbon source. When the flow rate was increased (under constant light intensity and CO_2 percentage) the growth rate increased while the volumetric production remained unchanged. An increased in light intensity resulted in an increased growth rate and volumetric production. A low inoculum achieved best antibiotic production as it produced more actively growing cells containing higher amounts of antibiotics (Chetsumon *et al*., 1994).

Anabaena variabilis has been used for hydrogen photoproduction while immobilized in a hollow fiber photobioreactor. The hollow fiber photobioreactor was run continuously for over a year (previously it had been used for five months on a continual basis) after inoculation with the cyanobacterium. 25^{o}C was optimal for H_2 production without CO_2 evolution (which

led to an increase in O_2 evolution). The photobioreactor was designed such that the growth medium passes from the outside of the hollow fiber (HF) into the inner lumen space. The adhesion of the bacteria to the membranes was tested in batch cultures prior to the construction of the bioreactor. Cells were immobilized on pieces of hydrophilic cuprammonium rayon hollow fibers (AM 100L) and hydrophobic polysulfone hollow fibers. AM 100L was used for the photobioreactor as microscopic examination revealed that the cells invaded all the spaces in the 15ml column. (Markov *et al.*, 1993 and Markov *et al.*, 1995).

Cells from the plant *Gossypium arboreum* were immobilized on a cotton matrix for the production of an anti-fungal compound, gossypol. The process was made continuous with the addition of a cell wall permeabilizer (DMSO) and addition of an elicitor increased secondary metabolite production 8-fold. The overall productivity was 20-fold higher than batch culture (Choi *et al.*, 1995).

1.5 The gradostat concept

It has been shown that nutrient gradients are established in biofilms of immobilized microorganisms. The profile of the nutrient concentration versus the distance from the biofilm is dependent on 1) microbial substrate uptake rate, which is a function of microorganism concentration and their affinities for the substrate 2) substrate transport rate through the biofilm, which is dependent on the substrate diffusivity and 3) substrate transport rate to the biofilm, which is a function of the microbial substrate uptake rate, substrate diffusivity through the biofilm and hydrodynamics near the biofilm surface.

Nutrient gradients have been shown to exist in hollow fiber bioreactors. Radial nutrient gradients are established around the lumen such that the cells closest to the capillary membrane surface receive the highest concentration while the cells on the outside of the biofilm are nutrient deprived. Additional nutrient diffusion resistance can be provided by extra-cellular product formation. The structure, activities and the composition of biofilms have been shown to change with biofilm depth.

These spatial concentration gradients may be exploited to produce secondary metabolites as secondary metabolism is usually triggered by nutrient deprivation. This concept is shown in Figure 1. New cells are continuously being formed at the base of the biofilm, pushing the older cells away to areas lower in nutrient concentration, which will trigger secondary

metabolite production. The cells producing the secondary metabolites may then be sloughed off with water or air shear.

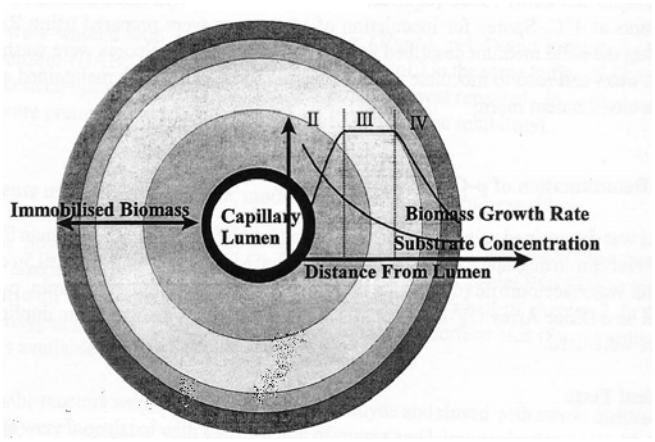

Figure 1.1: The gradostat concept (Burton *et al.*, 1998).

The added benefit to this system is that the nutrient supply is effectively sterilized by the filtrating effect of the pores that exist on the inner side of the lumen. The membrane (IPS 768) is specially produced to have an internal skin and a skinless outer membrane. The spongy outer membrane wall facilitates the attachment of spores or bacteria, due to its increase in surface area. In use for fungal spore attachment the time to adsorb was cut down from days with conventional outer skinned membranes to thirty minutes with IPS 768. The increased surface area also allows for denser biofilms to develop. (Burton *et al*., 1998)

By immobilizing bacteria on membranes it is possible to manipulate their environment such that a particular nutrient concentration can be achieved at extra-capillary membrane surfaces, allowing for a nutrient concentration that decreases from the interior to the exterior of the biofilm. A light gradient can be created in the opposite direction to the nutrient gradient as a function of the cell density. *Microcystis aeruginosa* PCC7806 secondary metabolite (microcystin LR and microcystin DaspLR) production is modulated by nutrient and light ratios and concentrations/intensities. Capillary membrane modules would allow fine-tuning of such ratios and concentrations within the biofilm thus allowing for control of secondary metabolite production. An additional advantage of the capillary membranes is that the waste products may be removed from the extracapillary space and the nutrient supply may be constantly maintained at its original concentrations. By immobilizing the cyanobacteria and adjusting the available concentrations of light and nutrients it may be possible to control the conditions in the outer layer of the biofilm such that a constant state may be maintained where microcystin production is at the maximum attainable level for this strain of *M.*

aeruginosa. Theoretically cell division should occur closer to the membrane, where nutrient levels are higher, and microcystin production will occur in the outer biofilm, where the light concentration is the higher and nutrient concentrations lower. The membrane reactor could therefore serve as an experimental tool to study biofilms of cyanobacteria in simulation of their natural environment, where they occur as biofilms and exposed to opposing nutrient and light gradients.

1.6 Objectives

The objectives of this project are listed as:

- Development of a module and inoculation technique that would allow for the efficient and aseptic immobilization of *Microcystis aeruginosa* PCC7806 upon an externally skinless polyethersulfone capillary membrane.

- The production of microcystin was to be assessed under immobilized conditions with variations of parameters such as light intensity, nitrate concentration, length of time of immobilization and biofilm thickness.

- The evaluation of the membrane bioreactor as an experimental tool to study the physiology of microcystin production in biofilms.

CHAPTER 2
MODULE DEVELOPMENT AND CELL IMMOBILIZATION

2.1 Introduction

A module and an inoculation technique had to be developed that would allow for the efficient immobilization of *Microcystis aeruginosa* PCC7806. A variety of module types with differing diameter, length and extra-capillary space volume were assembled. These were inoculated with the bacteria in order to obtain a stable biofilm in a suitable environment for toxin production. Methods of cell immobilization that were applied in this study included adsorption, pressure filtration and a newly developed technique that involved drying a cell slurry on the membrane.

2.2 Methods and Materials

2.2.1 Strains and culture conditions

Two *Microcystis aeruginosa* PCC7806 cultures were obtained from the University of Port Elizabeth, one in an exponential growth phase suspension, the other as colonies on a BG-11 agar plates. Both were used as inocula for an airlift reactor using BG-11 liquid growth medium. The cells were grown in airlift reactors at a temperature of 25^{o}C at a light intensity of 700 lux. These cells were used as inocula for the membrane modules.

2.2.2 Sample preparation for SEM

Samples were left in phosphate buffered saline (pH 7.05) containing 2.5% gluteraldehyde for 3 hours, freeze dried and gold coated in a Nanotech SEMPREP 2 Sputtercoater for 2.5 minutes at 0.1 torr at a current of 20 mA, and viewed and photographed with a Philips XL30 scanning electron microscope.

2.2.3 Externally skinless polyethersulfone capillary membrane module

The externally skinless polyethersulfone capillary membrane was obtained from the University of Stellenbosch. A membrane portion was cut to a length just longer than the module. A section of glass tubing was glued to either end with epoxy resin and allowed to harden for 20 minutes. The glass tubes were inserted through rubber seals at either end of the module and caps were screwed over both ends to provide a pressure-resistant seal. The module was left overnight to allow for the resin to set properly, sterilized with a 4%

formaldehyde solution (recirculating through the extra-capillary space as well as the lumen for four hours), and rinsed by flushing the module with autoclaved de-ionized water for three hours. Modules could not be autoclaved as the resin would disintegrate.

Pasteur pipettes were used to create alternative bioreactors as their thickness allowed for the passage of a red-hot pin to create an ECS inlet and outlet port and the tips could be modified to the outer diameter of the capillary membrane. Two of these modified pipettes were joined in the centre with a small portion of clear silicone tubing and the membrane was glued to the tips with resin an hour after inoculation. Water would be introduced to the ECS seven hours after the resin had been applied.

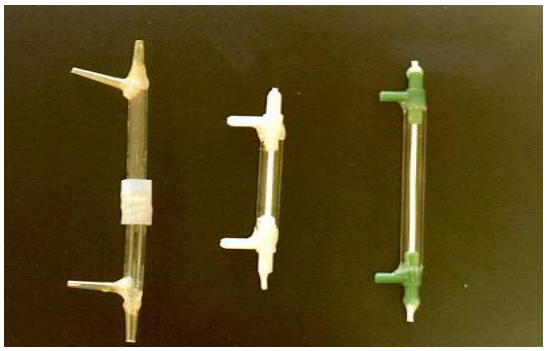

Figure 2.1: Different modules developed for this research. From left: MPP module, 5cm CM module and 8cm CM module.

The majority of the work done with this membrane was done using CM modules, (The different modules are shown in figure 2.1). They comprised of 2 aquarium t-joint adapters, which were glued with resin to either end of glass tubing (internal diameter of 5 mm and outer diameter of 7.2 mm), with lengths varying from 5 to 35 cm. A length of membrane was passed through and glued in while under tension. After 24 hours the resin was suitably hardened and the module was sterilized with 4% formaldehyde and flushed with sterile de-ionized water. A schematic depiction of a typical inoculated CM module is shown in Figure 2.2.

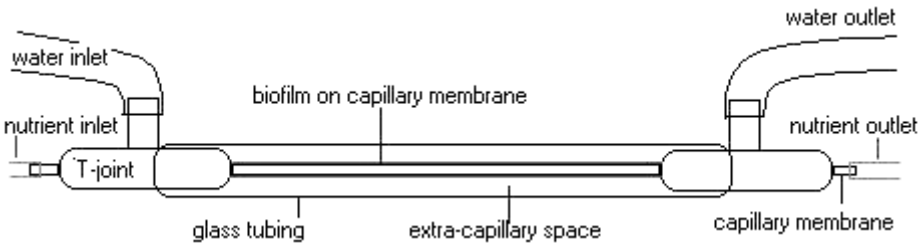

Figure 2.2: Schematic of the components of an inoculated CM module.

2.2.4 Methods of Immobilization

Adsorption

Adsorption was the first attempted method of biofilm attachment. One litre of a cell suspension with a cell density of 8 x 10^8 cells.ml^{-1} was re-circulated through the ECS at a flow-rate of 1 ml.min^{-1} for an hour and then flushed with distilled water.

Cell slurry immobilization

A cell suspension was centrifuged to a pellet and then mixed with a small quantity of water. This was drawn out in a line and a portion of membrane was rolled in the cell slurry until completely surrounded by a thick layer of cells and the biofilm was allowed to dry slightly before the membrane was glued into a module.

Pressure inoculation

Cells were pressure inoculated under aseptic conditions by filling the ECS with a concentrated cell suspension (2 ml for every 1 cm of membrane with cell number varying from 10^{11} to 10^{12} cells.ml^{-1}), blocking the outlet port, and increasing ECS pressure using a peristaltic pump. The membrane acted as a filter, trapping the cells on the shell side and letting the medium pass through to the lumen. Cells were immobilized by forced adhesion to the membrane. Loose aggregates were removed after inoculation by flushing de-ionized water through the ECS at 0.5 to 1 ml.min^{-1}. BG-11 medium was pumped through the lumen with a peristaltic pump at 0.5 ml.min^{-1} every 24 hours. The pressure increase during inoculation was monitored with a gauge that had a maximum reading of 400 kPa, although the pressure was not allowed to exceed 120 kPa.

2.3. Results

2.3.1 Adsorption

When the membrane was visually examined it was evident that adsorption was not a feasible form of immobilization. Cells had formed a thin biofilm on the top half the membrane as a result of deposition (the module had been standing horizontally), while the lower half of the membrane was devoid of any green colour that would have been imparted by cyanobacterial adhesion.

2.3.2 Cell slurry immobilization

Cell slurry immobilization on the externally skinless polyethersulfone membranes resulted in a thick (although uneven) biofilm and minimal loss of cells after inoculation. Cells penetrate the pores, but there were portions of membrane with no pore penetration (Figure 2.3a and 2.3b).

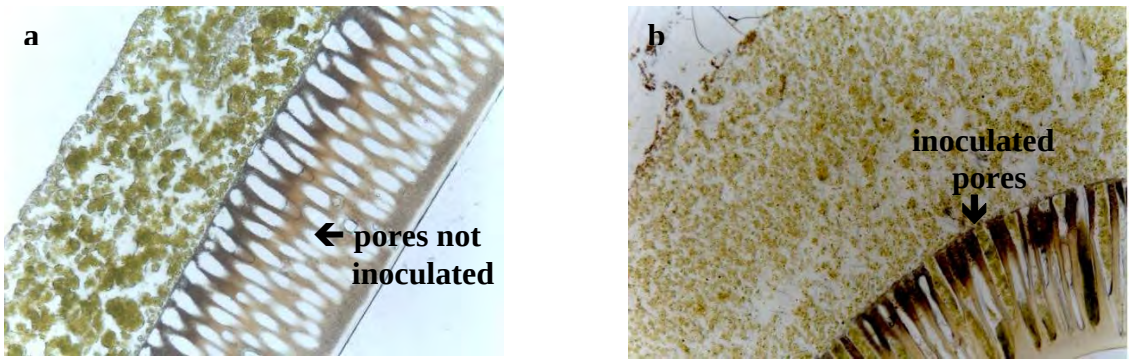

Figure 2.3: Wax embedded cross-sections of the cell-slurry attached biofilms with a) no pore penetration and b) biofilm with pore penetration (magnification 256 times).

Approximately 8 hours was optimal for adsorption at room temperature and ambient pressure, before the introduction of water into the ECS, as cells were well adsorbed to the membrane and one another. When the biofilm was desiccated it would crack and flake off as soon as water was introduced into the ECS. If the biofilm was still too moist the cells would wash off with the introduction of water into the ECS.

The technique required a sterile environment to work in, as contaminants were easily introduced. The uneven biofilm formation and inconsistency of the externally skinless membrane were a problem, as cells overlaying an inconsistent portion of the membrane (Figure 2.3) would not receive the same quantity, if any, nutrients. These inconsistencies would result in varying nutrient gradients along the length of the membrane and the data would not be consistent.

2.3.3 Pressure immobilization

Pressure immobilization led to the formation of thick biofilms in a relatively short period of time (20 to 40 minutes). Figures 2.4 and 2.5 show that the cells could penetrate well within the pores and a dense biofilm formed on the outside of the membrane. However, pore penetration was inconsistent.

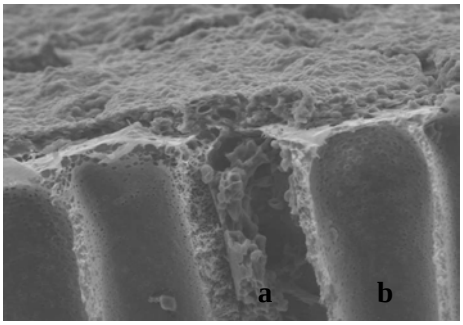

Figure 2.4: An inoculated externally skinless polyethersulfone membrane that was in a CM module showing a) an inoculated pore and b) an uncolonized pore at a magnification of 465 times.

Figure 2.5: a) SEM of biofilm formation at the outer surface and b) within the pores themselves. Both at a magnification of 465 times.

Complete biofilm formation could be seen on the one side of the membrane in Figure 2.6a and 2.6b, but uncolonized portions were evident in Figure 2.6c. Portions that did not have complete biofilm coverage were typically along one side of a length of membrane and occurred in oval patches. Some uncovered portions would form around the entire circumference of the capillary membrane. Scanning electron microscopy revealed that the inconsistencies were due to either the presence of an external skin, presence of a thick internal skin, poorly formed pores or a combination of these factors.

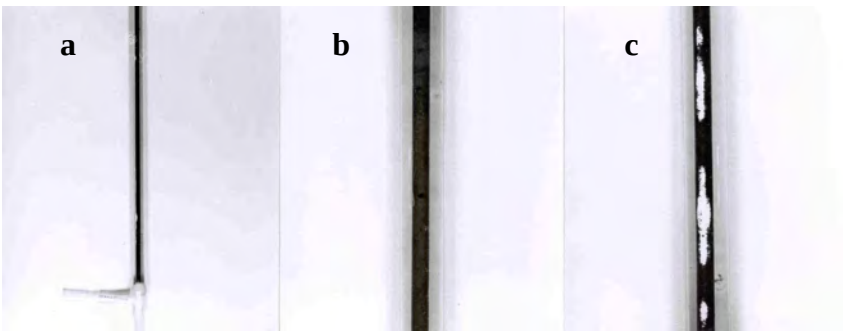

Figure 2.6: CM module directly after inoculation showing a a) portion of CM module, b) completely covered externally skinless membrane and c) incompletely covered externally skinless membrane.

The externally skinless polyethersulfone capillary membrane and the CM module were inexpensive and the module could be reused several times. The membrane could be cut to size easily and, with the use of adapters, fitted into a variety of modules. With the CM modules the lowered volume of the ECS meant fewer cells were lost in the inoculation process. Modules containing this membrane possessing a larger ECS lost a large percentage of cells in the inoculation suspension, as aggregates formed in solution before being immobilized to the membrane surface. These aggregates formed precipitates that did not adhere to the biofilm and had to be flushed out. A problem with a lowered ECS was that some aggregates could not be removed, as they were partially joined to the biofilm. The disadvantage was the membranes' low thermotolerance, which led to a longer chemical sterilization process, followed by flushing with sterilized de-ionized water to remove chemical traces. The major problem with the membrane was its inconsistency with regards to immobilization due to manufacturing inconsistencies.

Of the three immobilization techniques pressure filtration immobilization produced the best results in the fastest time. Biofilm formation was complete within 20 to 40 minutes and sterile conditions were maintained with relative ease. An advantage of this technique was that cells were immobilized according to suspension medium flux from the ECS into the lumen, which meant that poorly developed portions of the membrane did not allow for the cell suspension medium to pass through, and therefore did not allow for significant cell immobilization to occur. Cells were therefore not immobilized at the inconsistent portions of membrane, which occurred using the cell slurry immobilization technique. Although the cell slurry immobilization technique did produce a thick biofilm, it took a comparatively longer time, was inconsistent in thickness and contaminants were easily introduced. Adsorption was not feasible due to the low quantity of cells that adhered to the membrane.

CHAPTER 3

PHYSIOLOGICAL PROPERTIES THAT AFFECT IMMOBILIZATION OF *MICROCYSTIS AUREGINOSA* PCC 7806

3.1 Introduction

During module development cells would frequently immobilize poorly to the externally skinless polyethersulfone membranes, which was attributed to differing hydrophobic properties between membrane batches or cell cultures. In earlier protocols membranes would be rinsed with warmed water to remove any residual glycerol that would affect surface properties. After rinsing the CM modules with water heated to 45^{o}C attempts at cell immobilization failed again. Poor adhesion was thus attributed to physiological properties of the bacterial cultures such as the presence of gas vesicles and extracellular polysaccharide production. Cell cultures that adhered poorly were buoyant, while those that adhered well settled out of suspension relatively quickly. A review of available literature indicated that the cell surface properties, presence of gas vesicles and other intracellular substructures could affect the ability of the *Microcystis* cells to bind to membrane.

The surfaces of microbial cells are vital to the organism's survival, as it is through their surfaces that the bacteria interact with the environment. The cell surface can be covered with extracellular polysaccharide layer, which is either closely associated with the cell wall or exists as a loosely attached amorphous layer. Most extracellular polysaccharides located on the cell surface are synthesized from intracellular nucleoside diphosphate-sugar precursors, and must be transported through the cell membrane to the outside of the cell (White, 2000).
Some bacteria contain specialized organelles in the cytoplasm that are referred to as inclusion bodies. They differ from eukaryotic organelles in that they are not surrounded by a lipid-protein bilayer membrane, although they do have a membrane coating. Some of the regularly occurring inclusion bodies are DNA, ribosomes, glycogen, thylakoid membranes with associated phycobilliproteins, glycogen (α-granules), lipid inclusions (β-granules), cyanophycin granules (structured granules), polyhedral bodies (carboxysomes) and polyphosphate bodies (Jensen, 1985;White, 2000).

Gas vesicles occur in aquatic bacteria such as the cyanobacteria. They vary in size and consist of assemblages of hollow, cylindrical, proteinaceous structures. Their function is to alter the cell density, thereby allowing for vertical movement in the water column, in response to optimal temperature, light or nutrient concentrations. They are relatively small and are

required in large numbers (estimated to require approximately 10 000 gas vesicles per cell) for efficient buoyancy. These vesicles are ordered into gas vacuoles to occupy minimal space, and in this configuration provide optimum buoyancy. Factors shown to affect gas vesicle production are the availability if inorganic carbon, nitrogen and phosphate, and water temperature. The application of gentle pressure shrinks the gas vesicle imperceptibly, but an excessive hydrostatic pressure collapses it, and the cells lose buoyancy. The larger the gas vesicle the greater the pressure required to collapse it. Collapsed vesicles do not recover and cells can only acquire new vesicles through de novo synthesis (Romans and Carpenter, 1994; White, 2000 and Walsby *et al*., 1999).

Not all cyanobacteria rely solely on gas vacuolation for vertical movement. *Oscillatoria* and *Microcystis spp*. have been shown to regulate their position in the water column by carbohydrate accumulation and a decrease in gas vesicle number. In a further study *Microcystis* colonies were observed to regulate depth by co-precipitation with iron-laden colloids (Berner, 1993).

The photosynthetic membranes of cyanobacteria are intracellular membrane-bound sacs called thylakoids, which contain both reaction centers as well as light-harvesting complexes called phycobillisomes. The characteristic blue-green and red colours reflect the presence of the phycobillisomes, which are water-soluble light- harvesting antenna complexes that share similar tertiary and quaternary structures. The photosynthetic pigments are divided into two categories, which are the reaction center pigments (chlorophyll a: λ_{max} 680 nm) and light harvesting pigments (carotenoids, phycobillins and chlorophylls). Phycobilliproteins are the major components of these complexes and can represent 40% of the total protein present in cyanobacteria cultured under low light intensities. The three major classes of phycobilliproteins are phycoerythrins (λ_{max} 565 nm), phycocyanin (λ_{max} 620 nm) and allophycocyanin (λ_{max} 650 nm). Allophycocyanin is the major building block of the core of the phycobillisome. Radiating out from the core are rods composed of phycocyanin-linker polypeptide complexes. In some cyanobacteria phycoerythrin forms the distal portion of the rods (Schluchter and Glazer, 1999). Cyanophycin granules are storage granules composed of a polypeptide copolymer consisting of arginine and aspartic acid. They vary in size and number as a result of different growth conditions. They generally have a mottled appearance under the TEM (Jensen, 1985 and Schluchter and Glazer, 1999).

The objective of this chapter was to establish the immobilization potential between buoyant and non-buoyant cells and to verify if immobilized growth altered the physiology of *Microcystis aeruginosa* PCC 7806.

3.2 Methods and materials

3.2.1 Immobilization of buoyant and non-buoyant cells in CM modules

A cell suspension, containing buoyant cells, that had been cultivated in an airlift reactor was poured into a 250 ml graduated cylinder and left for 12 hours in a controlled environment room at 25^{o}C. The upper 100 ml (buoyant cells) was collected in a beaker and the remaining liquid was poured out until only settled (non-buoyant) cells remained, which were also collected. The cells were analyzed at various dilutions in a Microtitre plate reader (Biotek Instruments) at a wavelength of 740 nm, and a spectral scan from 400 to 700 nm was performed on wells with similar OD_{740} readings. The buoyant and non-buoyant samples were concentrated to similar OD_{740} readings (deviation of 0.008) and filtration-inoculated in CM modules. Photographs of the immobilized cells were taken while the cells were still under pressure (50 kPa) and 30 seconds and 12 hours after pressure cessation to demonstrate the dispersion of cells back into the liquid medium. Samples of cells were removed before and after the immobilization procedure for TEM processing.

3.2.2 Transmission electron microscopy (TEM)

Samples from the buoyant and non-buoyant cells, before and after inoculation, were washed with de-ionized water and processed for gas vesicle staining according to protocol by Romans *et al* (1994). Cells were washed in phosphate buffered saline (PBS) at a pH of 7.4, fixed in PBS containing 2.5% gluteraldehyde for an hour at 4^{o}C, post-fixed in a 1% OsO_4 solution for 2 hours. A portion from a week old biofilm was fixed in PBS containing 2.5% gluteraldehyde overnight. All five samples were dehydrated in a graded ethanol series and immersed twice for 10 minutes in 100% propylene oxide. Samples were infiltrated with resin through a graded resin: propylene oxide mixture (25:75, 50:50, 75:25 for 90 minutes), left in pure resin overnight, placed in fresh resin for 6 hours and then baked in an oven at 60^{o}C for 48 hours. Sections were cut with glass blades and stained with uranyl acetate (4%) and lead citrate before being examined and photographed under a TEM.

3.2.3 Scanning electron microscopy (SEM)

A sample from a week old biofilm was fixed in PBS containing 2.5% gluteraldehyde overnight, freeze dried, frozen in liquid nitrogen, cut transversely across the membrane, fixed to a stub with colloidal silver, gold-coated in a Nanotech SEMPREP2 sputtercoater for 2.5 minutes at pressure of 0.1torr at a current of 20 mA, viewed and photographed with a Philips XL30 scanning electron microscope.

3.2.4 Light microscopy

A sample from a week old biofilm was fixed in PBS containing 2.5% gluteraldehyde overnight and freeze-dried. The sample was immersed in molten paraffin wax for 2 minutes (with gentle shaking to remove all air bubbles) and allowed to set in an aluminium-foil mould that was fixed to a wooden block. The wooden block was clamped into a microtome and samples were cut parallel to the membrane in 8 μm sections. Portions of the wax ribbon were selected such that cells in the outer, middle and inner biofilm were represented. Sections were examined and photographed under an Olympus BX60 light microscope.

3.3 Results and Discussion

From Figures 3.1, 3.2 and 3.3 it was evident that differences in physical properties such as cell density had an impact upon the potential of the bacteria to be immobilized on a synthetic membrane.

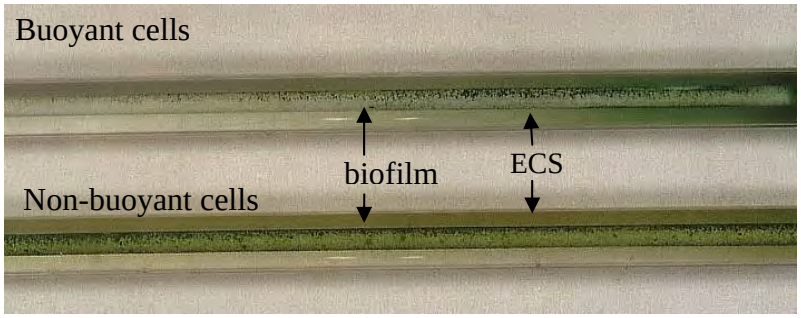

Figure 3.1: Biofilms of Buoyant and Non-buoyant *Microcystis* cultures showing better attachment of non-buoyant cultures while still under pressure (50 kPa).

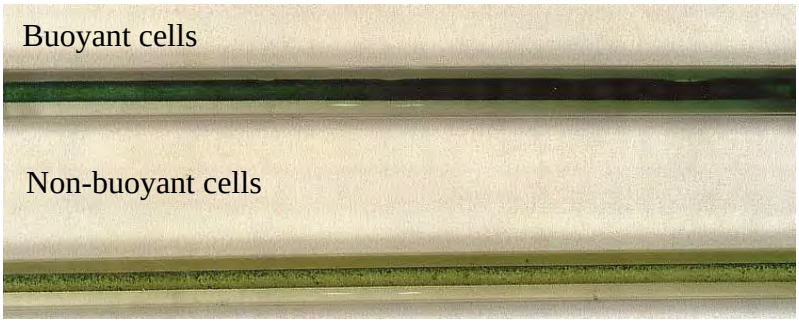

Figure 3.2: Biofilms 30 seconds after pressure inoculation was stopped.

Figure 3.3: Biofilms 12 hours after pressure inoculation was stopped, showing re-suspension of the Buoyant cells.

Buoyant cells rapidly dissociated from the membrane into the surrounding medium. Settling was attributed to the immobilization pressure being sufficient to destroy smaller gas vesicles, which increased cell density to the point where they were no longer buoyant. A second attempt to immobilize the buoyant cells, which had settled after the immobilization, failed. This indicated a second reason for lack of adherence, which only became evident once the cells were observed under a TEM.

Figures 3.4 and 3.5 showed the buoyant and non-buoyant cells to be of equal dimensions, but there were morphological differences between them.

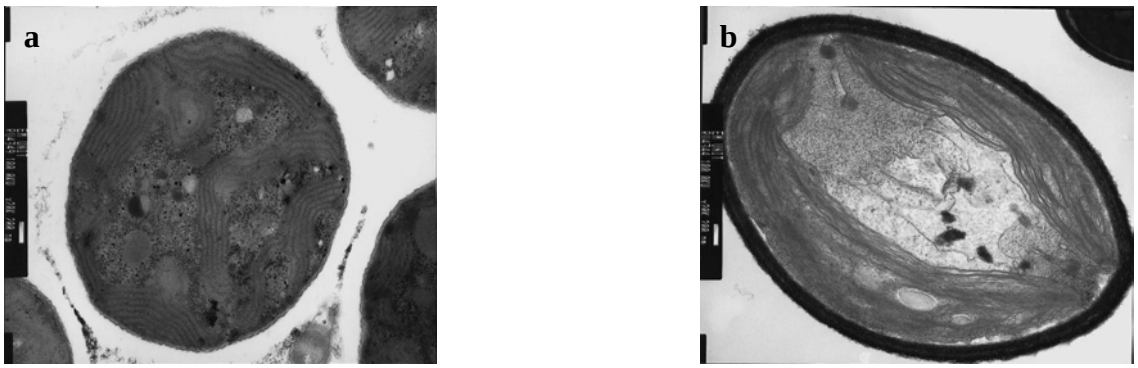

Figure 3.4: TEM of a) buoyant (magnification at 8570 times) and b) a non-buoyant cell (magnification of 9850 times).

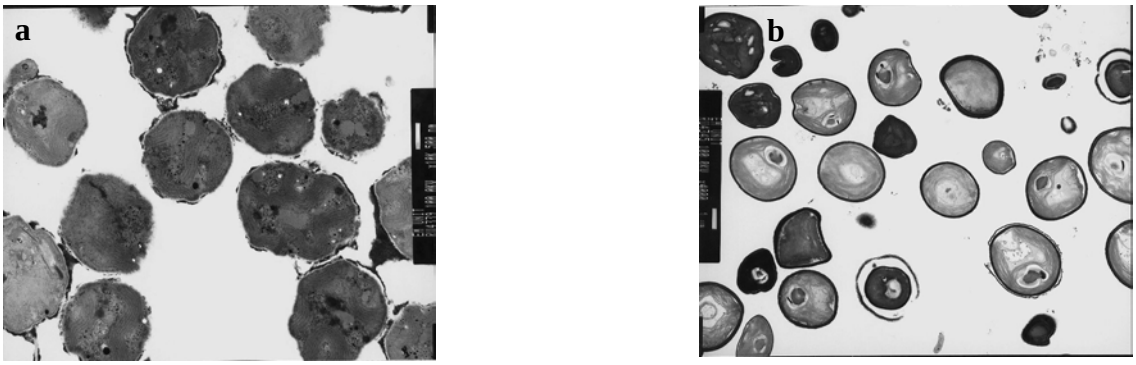

Figure 3.5: Array of a) buoyant cells (cell walls ill-defined) and b) non-buoyant cells (well-defined cell walls) before inoculation (at a magnification of 4280 and 1720 times respectively).

The non-buoyant cells had thick, structured walls, compacted thylakoid networks and a low cyanophycin content. Buoyant cells had a more dynamic, less structured cell wall, dispersed thylakoid networks, and a number of inclusions. The buoyant cells appeared to be in a state of division (more evident in Figure 3.8b)

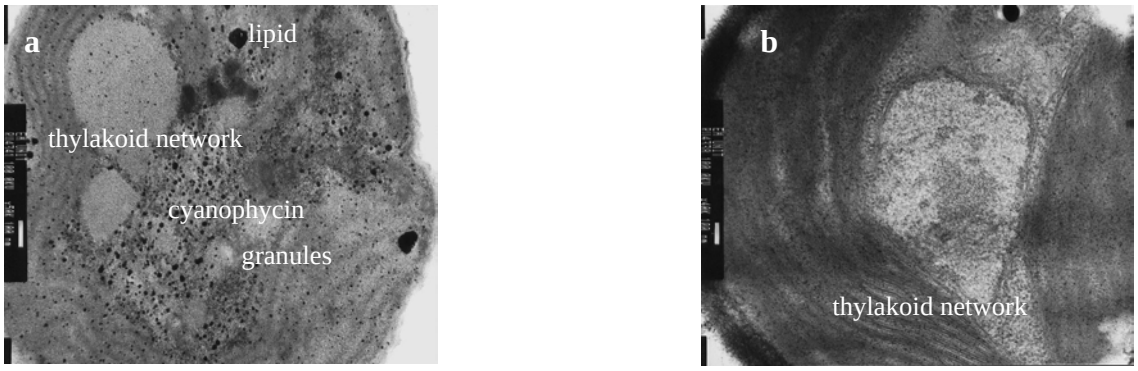

Figure 3.6: TEM of a) buoyant cell and b) a non-buoyant cell (both at a magnification of 21400 times).

The mottled appearance inside the cell (Figure 3.6a) and a larger peak at 615 nm in the spectral scan (Figure 3.7a) were indicative of phycocyanin granules. The dense black specks were lipid inclusions.

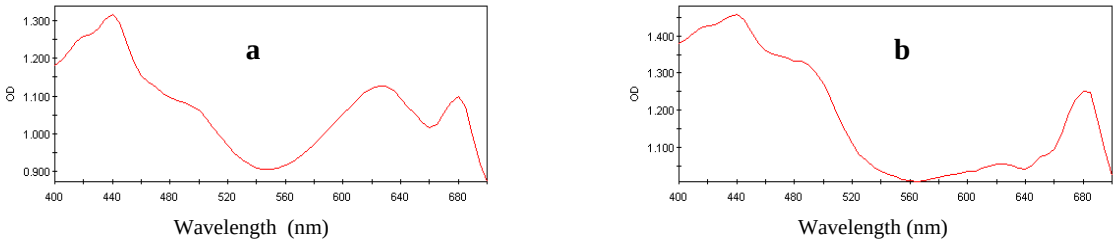

Figure 3.7: Absorption spectrum from 400 to 700 nm for a) buoyant cells and b) for non-buoyant cells. The buoyant cells had a much greater peak at 615 nm.

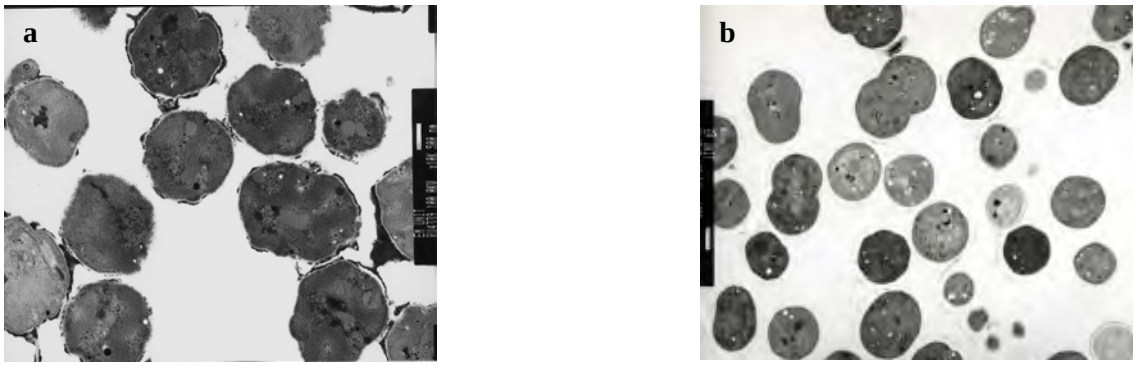

Figure 3.8: Buoyant cells a) before and b) after immobilization (at a magnification of 4280 and 1720 times respectively).

The cell walls of the buoyant cells were altered by the immobilization procedure. Figure 3.8a and 3.8b showed the majority of the EPS to be missing from the cells after inoculation. It was possible that the EPS was poorly attached to the bacteria and was removed by cell-cell or cell-membrane interaction during inoculation. This lack of adherent material may have prevented the cells from immobilizing with the second attempt, which was done using cells from the buoyant culture that settled after the first immobilization procedure.

No gas vesicles were evident in the stained buoyant cells (Figures 3.4a, 3.5a, 3.6a, 3.8a and 3.8b).

The bacteria did not show external morphological differences across the biofilm under the highest magnification of the light microscope, as indicated by Figure 3.9a, b and c. Sections were cut parallel to the lumen.

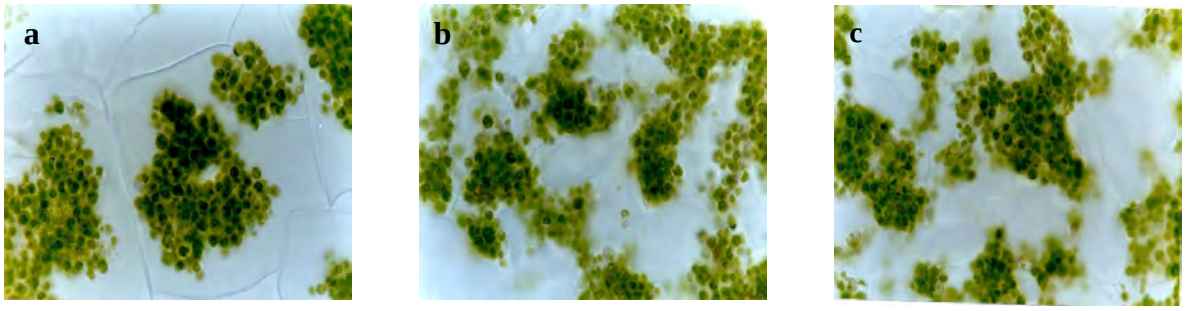

Figure 3.9: Cell morphology a) near to the membrane b) 16 µm into the biofilm and at the c) outer biofilm layer (light microscopy: magnification 246 X).

A transverse SEM (Figure 3.10) displayed what might have been a physiological adaptation to immobilization, in that cells were slightly ovoid parallel to the membrane. This would represent a more disc-like shape, which would increase the cell's surface area and efficiency of harvesting light.

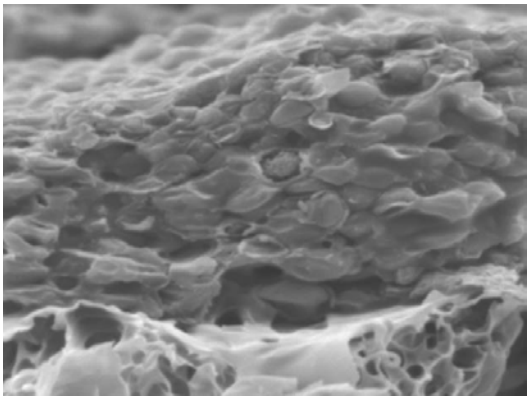

Figure 3.10: SEM of a transverse profile of the cyanobacteria across the biofilm (at a magnification of 760 times).

A transverse section of the cells in the biofilm from its base to the outer cells, under TEM, would have been ideal in order to establish how internal and external cellular morphology was affected by membrane immobilization, but sample processing for the TEM adversely affected the membrane. As a result TEM sections were cut in an attempt to locate cells in

pores, at membrane surfaces and in the outer biofilm, that were at that location in the original biofilm.

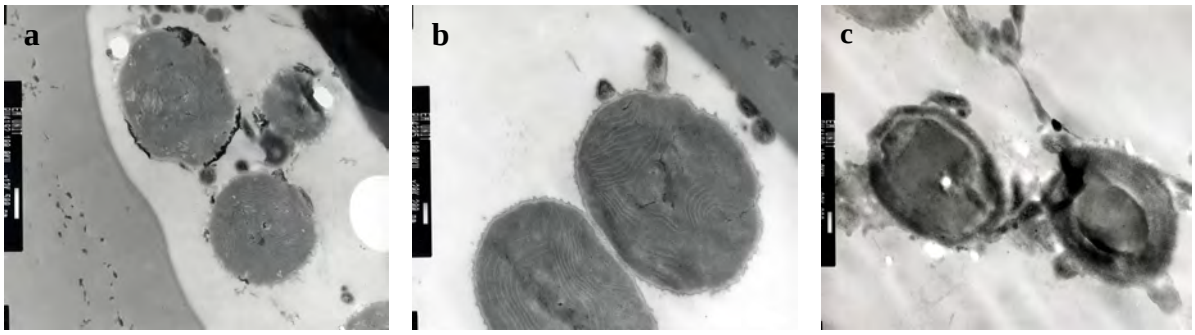

Figure 3.11: TEM showing a) morphology of cells within a pore b) morphology near capillary membrane surface and c) within the biofilm. At a magnification of 3900, 4600 and 3900 times respectively.

Cells within the pore and close to the membrane surface (Figure 3.11a and 3.11b) bore resemblance to cells shown in Figures 3.4a, 3.5a and 3.6a, indicative of an actively growing cell in a state of division. This would have been expected as these cells had the greatest amount of nutrients available to them. Figure 3.11c was located in the outer biofilm and possessed thick cell walls, resembling physiologically less active cells (shown in Figures 3.4b, 3.5b and 3.6b). Cells in Figure 3.11 appeared to have EPS extensions associated with them. They might have been physiological adaptions to aid attachment or cell debris from cells lysed during immobilization. Cell debris shown in Figure 3.12a and 3.12b was a fairly common occurrence in the micrographs. The micrographs show loose inclusions and EPS fragments.

Figure 3.12: TEM of cell debris at a magnification of a) 12100 and b) 14240.

3.5 Conclusions

The buoyant cells were in a rapid state of division and contained stores in the form of inclusions such as lipid globules and cyanophycin granules. The non-buoyant cells probably resulted from aggregate formation, which led to cells at the interior of the aggregate being nutrient stressed, thereby forcing use of their nutrient stores. They would also have had less exposure to light, hence the more compacted thylakoid network and evident decrease in accessory pigments.

Cells that were not buoyant and that possessed a more developed EPS layer immobilized more successfully. Buoyancy inhibited immobilization, as the lowered cell density resulted in forces of attraction to the surrounding medium that was greater than the forces holding the cell to the membrane and one another. The non-buoyant cells were used to determine the effect that immobilization had on toxin production under various parameters, and since they did contain microcystin, samples were taken at the time of immobilization to ensure that microcystin was being produced afterwards.

Cells within the pore and close to the membrane surface bore resemblance to cells in a state of active growth, as they had the greatest concentration of nutrients available to them. Cells in the outer biofilm possessed thick cell walls, resembling physiologically less active cells. EPS extensions may have been formed to aid adherence of cells in the biofilm or may have constituted cellular debris.

CHAPTER 4

TOXIN PRODUCTION

4.1 Introduction

After a reactor system and immobilisation procedure had been established for *Microcystis aeruginosa* and the question of cell buoyancy had been resolved, parameters that affected the microcystin production in free-living bacteria such as nutrient concentration, light intensity, and temperature, were to be assessed under immobilized conditions. Parameters tested were time, nitrate concentration, light intensity and finally biofilm thickness.

4.2 Methods and Materials

Table 4.1 represents an overview of the experiments in this chapter, describing the membranes used and the size of the modules they were used in. The end of this section decribes the method by which the membranes were inoculated and the biofilms sacrificed, as well as the methods for the protein phosphatase inhibition (PPI) assay and high performance liquid chromatography (HPLC) assay.

Table 4.1: Overview of experiments and membranes used. (ESCM: eternally skinless polyethersulfone capillary membrane)

Experiment	Membrane	Module size (cm)	Parameter assayed
4.2.1	ESCM	35	Time (30 days)
4.2.2	ESCM	35	Time (7 days)
4.2.3	ESCM	35	Biofilm thickness and nitrate concentration
4.2.4	ESCM	35 and 20	Time, light intensity, nitrate concentration and biofilm thickness
4.2.5	Free cells	Free cells	High light intensity with no nutrients

4.2.1 Assessment of toxin production over a 30 day period using ESCM in 35 cm CM modules

Ten 35 cm CM modules were inoculated with equal aliquots of a concentrated cell suspension. A peristaltic pump was used at a flow-rate of 0.5 $ml.min^{-1}$ to replace the BG-11 solution in the lumens of the reactors every 12 hours, and the ECS was flushed with de-ionized water at 0.5 $ml.min^{-1}$ every 24 hours. The experiment was conducted in a controlled environment room at 25^{o}C and a light intensity of 700 lux. Biofilms were sacrificed every 3

days and toxin production was quantified using the PPI assay. Figure 4.1 illustrates the assembly of the experiment.

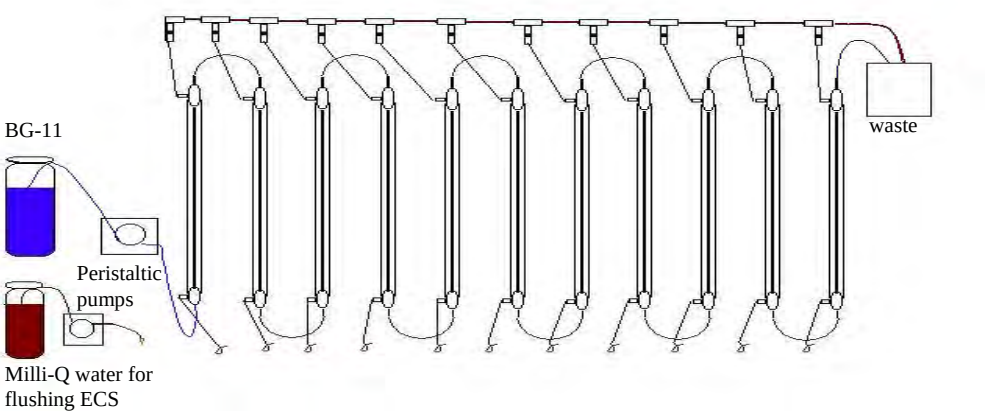

Figure 4.1: Diagram of module assembly for the 30-day experiment.

4.2.2 Assessment of toxin production over 7 day period using ESCM in 35cm CM modules

The experiment relating microcystin production to time was repeated over a period of seven days instead of 30. A peristaltic pump was used at a flow-rate of 0.5 $ml.min^{-1}$ to replace the BG-11 solution in the lumens of the reactors every 24 hours, and the ECS was flushed with de-ionized water at 0.5 $ml.min^{-1}$ every 24 hours. Biofilms were sacrificed every 24 hours and toxin production was quantified using HPLC.

4.2.3 Assessment of toxin production with various biofilm thicknesses over a 10 day period with two nitrate concentrations in ESCM in 35 cm CM modules

Sixteen modules were divided into two groups and inoculated with different volumes of a concentrated cell suspension to create biofilms with varying thicknesses. The lumens were flushed every 24 hours with either BG-11 at the normal nitrate concentration (20 mM) or $1/20^{th}$ of the normal nitrate concentration (1 mM). The ECS was flushed every two days with de-ionized water. The experiment was conducted at $25^{o}C$ at a light intensity of 700 lux and all biofilms were sacrificed after 10 days.

4.2.4 Full factorial experiment to determine the effects of time, light intensity, nitrate concentration and biofilm thickness on toxin production.

The experiment was a 4 X 2 factorial design that allowed for the investigation of the four major parameters affecting toxin production using 16 CM modules. The parameters are shown in Table 4.2.

Table 4.2: Parameters tested in individual modules in the matrix experiment

Module number	Light intensity (lux)	Time	mM nitrates in BG-11	Biofilm thickness
1	700	5 hrs	20 mM	thin
2	700	5 hrs	20 mM	thick
3	700	5 hrs	1 mM	thin
4	700	5 hrs	1 mM	thick
5	700	4 days	1 mM	thick
6	700	4 days	1 mM	thin
7	700	4 days	20 mM	thick
8	700	4 days	20 mM	thin
9	5900	5 hrs	1 mM	thin
10	5900	5 hrs	1 mM	thick
11	5900	5 hrs	20 mM	thin
12	5900	5 hrs	20 mM	thick
13	5900	4 days	1 mM	thin
14	5900	4 days	1 mM	thick
15	5900	4 days	20 mM	thin
16	5900	4 days	20 mM	thick

A moderate light intensity of 700 lux was standard in the controlled environment room in which the experiment was conducted, while a high light intensity was provided by a modified light box having fluorescent lights at each of its three sides. The intensity of the light emitted was measured at the central point in the light-box at every 90^{o}, and was found to be 6000 lux (from top), 5600 lux (from closed side), 6000 lux (from base) and 3000 lux (from open side). The light box had been constructed such that light intensity reaching the modules would be similar from all angles.

Times that were assessed were 5 hours and 4 days. It had been suggested that cyanobacteria could start producing secondary metabolites within 4 hours of immobilization, and that continuous cultures in a transition state had stabilized within 5 days (Wiedner *et al*., 2001).

The nitrate concentration was varied such that there was a relatively high and a relatively low concentration available to the bacteria. The BG-11 flushed through the lumen was used at the

normal nitrate concentration of 20 mM, and at 1 mM to simulate a nitrate-deficient environment. The lumens were flushed slowly by syringe every 24 hours, with care being taken not to impose any pressure that would affect the biofilm or increase the nutrient concentration in the ECS.

Two biofilm thicknesses labeled as either thick or thin were inoculated. The relatively thick biofilm was created by inoculating 20 ml of a concentrated cell suspension into a 25 cm module. The relatively thin biofilms were created by inoculating 15 ml of the same suspension into a 35 cm module.

4.2.5 Induction of secondary metabolite production by complete nutrient deprivation under a high light intensity.

Two cell cultures (buoyant and non-buoyant) were centrifuged, washed twice and suspended in de-ionized water. 10 ml samples were pipetted into 25 ml conical flasks and placed under lighting at 5600 lux at 25^{o}C. Samples were taken at 0, 2, 4, 6, 12 and 18 hours and toxin content measured.

4.2.6 CM Module construction and biofilm inoculation

35 cm and 20 cm CM modules were assembled and sterilized using the technique described in Chapter 2. Membranes had to be glued in under tension, to prevent the membrane from sagging against the side of the glass tubing (due to swelling) during inoculation, as this adversely affected biofilm formation. The inoculum suspension was divided into equal volumes and inoculated using a peristaltic pump, with pressure not exceeding 120 kPa. The times taken to reach 120 kPa varied from module to module (attributable to membrane manufacturing inconsistencies) and this affected the quantity of cells immobilized. De-ionized water was flushed through the ECS until all cells had either been immobilized or had formed non-immobilized aggregates. Aggregates were flushed from the ECS with de-ionized water at a flow-rate of 0.5 ml.min^{-1}. The lumen was flushed and sealed with a nutrient medium (BG 11, shown in Table 1 and 2 in Appendix).

4.2.7 Biofilm sacrifice for CM modules

Cells were dislodged from the membrane by forcing de-ionized water across the membrane from the lumen to the ECS. Half the suspension was collected and the module was shaken vigorously. This was repeated five times and the resultant cell suspension was pelletted, freeze-dried, suspended in 70% methanol at 80 µl.solvent.mg^{-1} dry mass, sonicated and

extracted for three 24 hour periods (replacing the 70% methanol each time) while being shaken moderately. The solvent was removed by low-pressure evaporation and the extracts were suspended in either a buffer (for PPI assay) or 70% methanol (for HPLC).

4.2.8 PPI Assay

100 µl of the sample (which was evaporated and suspended in a buffer containing 50 mM Tris-HCl, 0.2 mM $MnCl_2$ and 20 mM $MgCl_2$ at pH 8.1), 50 µl of a 20 mM $MnCl_2$ solution and 100 µl of the substrate (para-nitrophenyl phosphate (pNPP) at a concentration of 20 mM in a buffer containing 50 mM Tris-HCl, 0.2 mM $MnCl_2$ and 20 mM $MgCl_2$ at pH 8.1), was pipetted into a 300 µl well on a 96-well plate. 50 µl of the buffered protein phosphatase (the buffer containing 50 mM Tris-HCl, 1 mM Na_2EDTA, 2 mM $MnCl_2$, 0.5 g.L BSA and 0.1%(v.v) B-mercaptoethanol at a pH of 7.4) was thawed, warmed rapidly to 37^{o}C, and added to the well. The change in absorbance at 410 nm was measured every 3 minutes over a half-hour period (Ward *et al*., 1997). A calibration curve was obtained using microcystin LR (Sigma). The toxin production was assayed using the PPI assay and HPLC. After obtaining the results for the 30-day growth experiment the toxin production was quantified using HPLC.

4.2.9 HPLC Assay

The mobile phase was a 60:40 acetonitrile:water solution used at a flow-rate of 1 ml.minute. A Waters C18 reverse-phase column with dimensions of 4.6 x 250 mm was used on a Beckman System Gold Programmable Solvent Module 126, with a Beckman System Gold Diode Array detector, using a single wavelength scan at 238 nm and a multi-wavelength scan from 200-300 nm. A calibration curve was obtained using microcystin LR (Sigma).

4.3 Results and Discussion

For this section biofilm thickness is represented as the cell dry mass (ng) divided by the biofilm-covered surface (mm^2). Specific yield of toxin is represented by total toxin produced (µg) divided by the dry mass of the cells (mg) and toxin production per unit area is expressed as total toxin produced (ng) divided by the biofilm-covered surface area of the membrane (mm^2).

4.3.1 Assessment of toxin production over a 30 day period using ESCM in 35 cm CM modules

Data (Figure 4.2) showed the toxin content per cell to increase over a thirty-day period. No distinct trend appeared with toxin production relative to area with increasing time. When the data was placed in order of increasing biofilm thickness (Figure 4.3) an increase in total toxin production per unit area of membrane was observed, while toxin content per cell remained similar. What was of importance with regards to Figure 4.3 and 4.5 was that biofilms of different ages were being compared. Two biofilms that had exactly the same biofilm density could not be compared if there was a large difference between their times of inoculation and sacrifice, as cells might still be adjusting their internal physiology according to the immobilized environment.

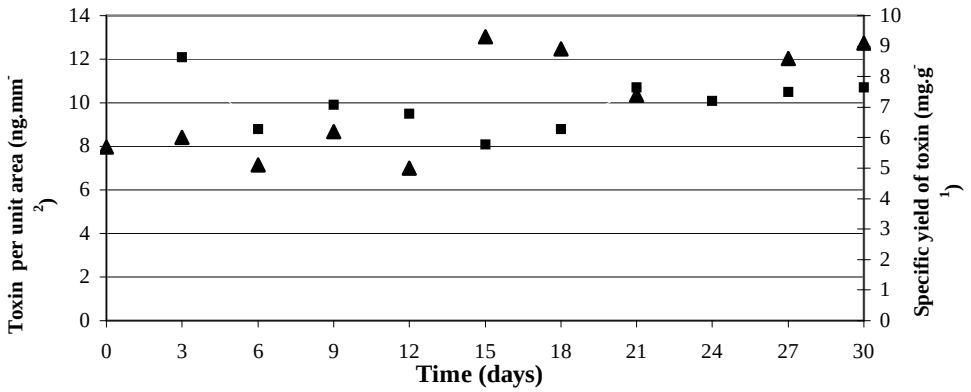

Figure 4.2: Comparison of the toxin production per cell and toxin production per unit area and biofilm thickness over a thirty day period determined by the PPI assay (Data from day 24 omitted). ▲: Specific yield of toxin ($mg.g^{-1}$) ■ : toxin production per unit area ($ng.mm^{-2}$). Data shown in Appendix in Table A.3.

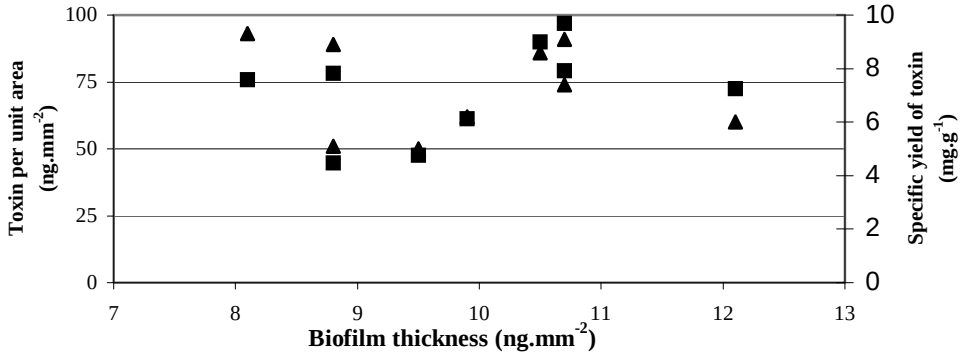

Figure 4.3: Specific toxin yield and toxin production per unit area plotted as a function of increasing biofilm thickness (data from day 24 omitted). ▲: Specific yield of toxin ($mg.g^{-1}$) ■: toxin production per unit area ($ng.mm^{-2}$) . Data shown in Appendix in Table A.3.

4.3.2 Assessment of toxin production over 7 day period using ESCM in 35 cm CM modules

Figure 4.4 showed toxin production to be erratic and did not conform to a trend when expressed as a function of time. Toxin content per cell appeared to increase, decrease, and then increase again. Toxin production relative to surface area appeared to decrease over the time period (Figure 4.5). The results could not be considered in isolation, as biofilm thickness appeared to play a pivotal role in the toxin production capacity per biomass, as well as per unit area of membrane. It was not possible to establish biofilms of equal thickness using the inconsistent externally skinless polyethersulfone membranes, which made experiments such as this very difficult to analyze due a primary factor in toxin production not being constant.

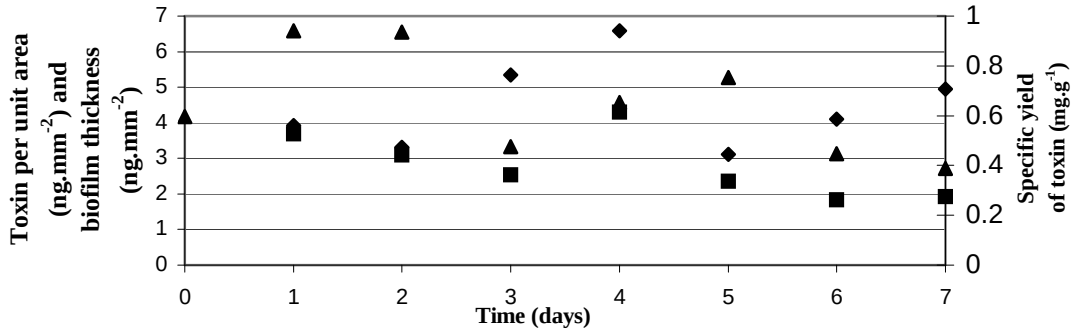

Figure 4.4: Specific toxin yield, toxin production per unit area and biofilm thickness over a seven day period. ▲: specific yield of toxin ($mg.g^{-1}$) ■: toxin production per unit area ($ng.mm^{-2}$) ♦: biofilm thickness ($ng.mm^{-2}$). Data shown in Appendix in Table A.4.

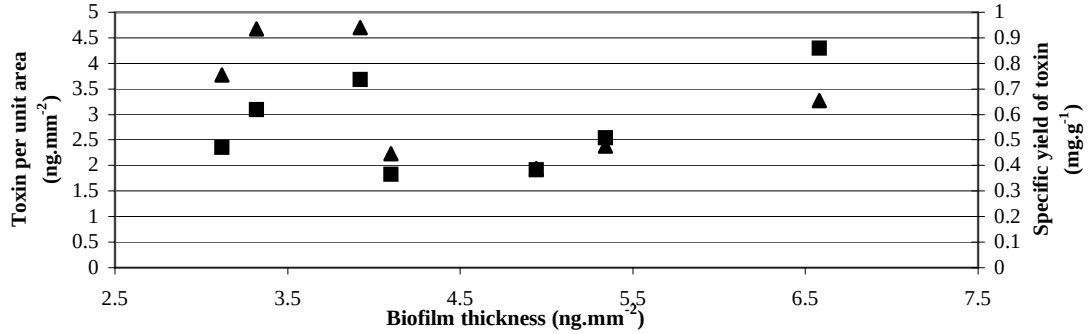

Figure 4.5: Specific toxin yield and toxin production per unit area plotted as a function of increasing biofilm thickness ($ng.mm^{-2}$).▲: Specific yield of toxin ($mg.g^{-1}$) ■: toxin production per unit area ($ng.mm^{-2}$). Data shown in Appendix in Table A.4.

4.3.3 Assessment of toxin production with various biofilm thicknesses for a 10 day period with two nitrate concentrations in ESCM in 35 cm CM modules

The aim of this experiment was to determine the affect biofilm thickness would have upon toxin production per cell as well as per unit area. The affect of two nitrate concentrations upon differing biofilm thicknesses was also assessed. Theoretically, if only a thin portion of

the biofilm was producing toxin, the thicker biofilms would have had a greater quantity of cells in the stationary phase of growth, and therefore a lowered specific yield of toxin. Figure 4.6a represents the biofilms exposed to a nitrate concentration of 20 mM and Figure 4.6.b represents the biofilms exposed to a nitrate concentration of 1 mM. Modules were placed in order of increasing biofilm thickness for each nitrate concentration.

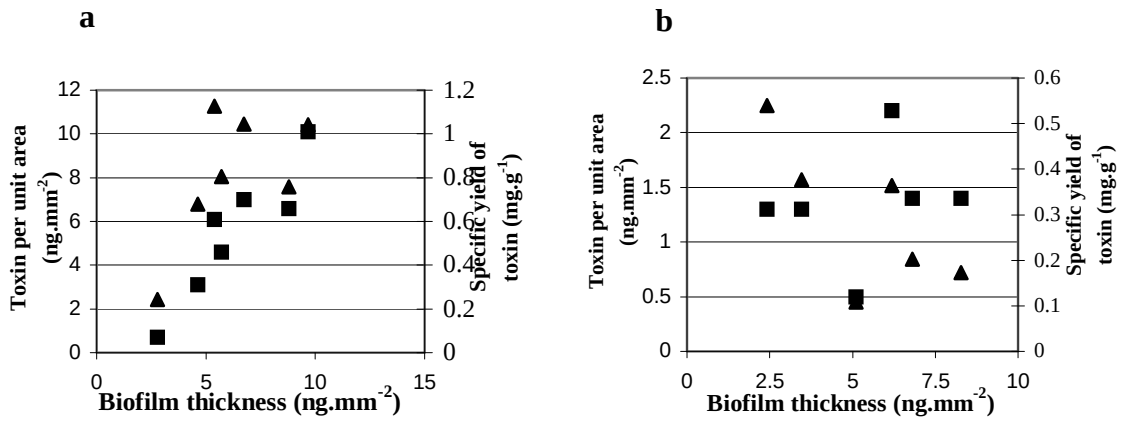

Figure 4.6: Specific toxin yield and toxin production per unit area plotted as a function of increasing biofilm thickness. (ng.mm^{-2}). **a)** Modules that had BG-11 at 20 mM nitrate concentration while **b)** depicts the results of modules that had BG-11 at 1 mM nitrate concentration. ▲: Specific yield of toxin (mg.g^{-1}). ■: toxin production per unit area (ng.mm^{-2}). Data shown in Appendix in Table A.5.

In Figure 4.6a the thinner biofilms (2.78 to 4.62 ng.mm^{-2}) displayed the lowest toxin content per cell. The nutrients available to cells were in excess such that cells were not nutrient stressed and therefore had a lowered microcystin content. Microcystin content per cell increased with a biofilm thickness from 5.4 to 9.68 ng.mm^{-2}, but the increase was not substantial relative to the increase displayed by cells in batch cultures from lag phase to late exponential growth phase. Toxin production per unit area showed a steady increase with increasing biofilm thickness. Theoretically, as the biofilm thickness increased further, a thickness would have been reached where a greater amount of cells would have been in the late stationary growth phase, which is less productive. The toxin content per cell would have decreased through biomass dilution and production per unit area would have eventually have leveled out. The efficiency of specific toxin production was not as important as total production of toxin per unit area of membrane, and thicker biofilms produced more microcystin per unit area.

With the lower nitrate concentration (1 mM) there was a lower microcystin content per cell (Figure 4.6b), which decreased as biofilm thickness increased. Although there was no trend observed with microcystin production per unit area relative to biofilm thickness, there was a

marked overall decrease relative to the cells exposed to 20 mM nitrates. The amount of nitrates reaching the bacteria was low and therefore used up quickly, not allowing for a proper nutrient gradient to be established. Even a thin biofilm (2.42 $ng.mm^{-2}$) could barely support toxin production at these lowered nitrate levels.

4.3.4 Matrix experiment to determine the effects of time, light intensity, nitrate concentration and biofilm thickness variation in biofilms

The matrix experiment was designed such that the predominant variables that affected microcystin production under immobilized conditions (time, nitrate concentration, light intensity, and biofilm thickness) could be tested in a relatively short time period using as few modules as possible. The data obtained is shown in Table 4.3.

Table 4.3: Parameters and results for the matrix experiment.

No	Light intensity (lux)	Time	$[NO_3^{2-}]$ (mM) in BG-11	Relative biofilm thickness	Biofilm thickness ($ng.mm^{-2}$)	Specific yield of toxin ($mg.g^{-1}$)	Toxin per unit area ($ng.mm^{-2}$)
1	700	5 hrs	20 mM	thin	3.64	1.887	6.89
2	700	5 hrs	20 mM	thick	5.84	0.488	2.85
3	700	5 hrs	1 mM	thin	2.75	0.479	1.32
4	700	5 hrs	1 mM	thick	7.76	0.398	3.09
8	700	4 days	20 mM	thin	2.80	1.249	3.50
7	700	4 days	20 mM	thick	8.29	0.564	4.67
6	700	4 days	1 mM	thin	3.42	0.653	2.24
5	700	4 days	1 mM	thick	7.45	0.648	4.83
11	5900	5 hrs	20 mM	thin	4.50	0.463	2.09
12	5900	5 hrs	20 mM	thick	5.98	0.568	3.39
9	5900	5 hrs	1 mM	thin	5.55	0.499	2.77
10	5900	5 hrs	1 mM	thick	9.55	0.514	4.91
15	5900	4 days	20 mM	thin	4.96	0.811	4.03
16	5900	4 days	20 mM	thick	9.88	0.293	2.90
13	5900	4 days	1 mM	thin	5.62	0.366	2.05
14	5900	4 days	1 mM	thick	9.15	0.608	5.56

The trend of increased production per unit area was evident when comparing data with regards to increasing biofilm thickness (Figure 4.7). Specific toxin production decreased and then levelled out as the biofilms became thicker.

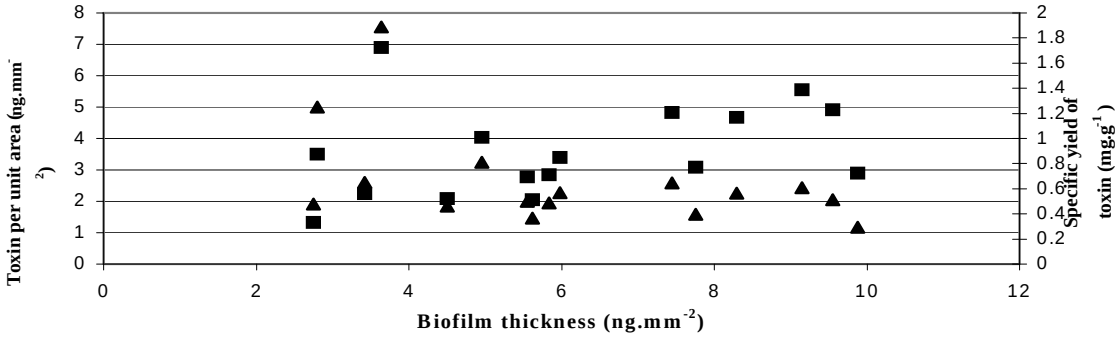

Figure 4.7: Specific toxin yield and toxin production per unit area plotted as a function of the biofilm thickness. ▲: specific yield of toxin ■: toxin production per unit area. Data shown in Table A.6.

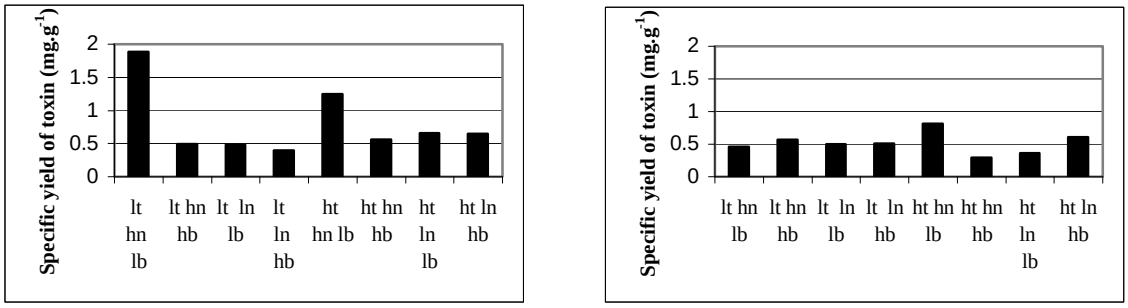

Figure 4.8: Specific yield of toxin for cells exposed to **left)** the lower light intensity and **right)** higher light intensity. ht: longer time on membrane. lt: shorter time period on membrane, hn: higher nitrate concentration, ln: lower nitrate concentration, hb: thicker biofilm, lb: thinner biofilm.

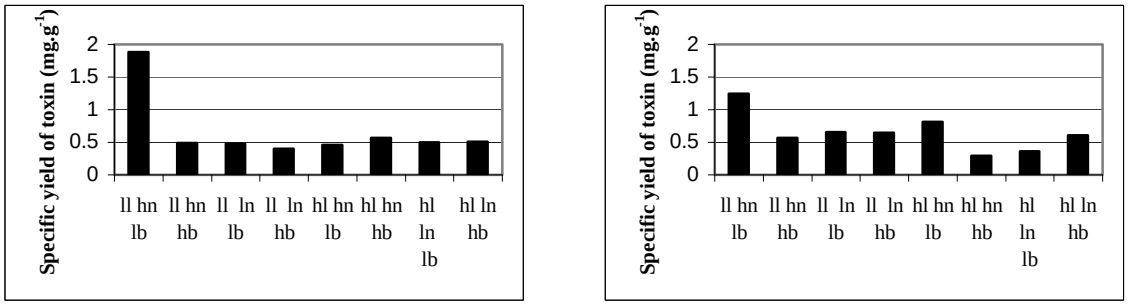

Figure 4.9: Specific yield of toxin for the cells immobilized for **left)** shorter time period and **right)** longer time period. hn: higher nitrate concentration, ln: lower nitrate concentration, hb: thicker biofilm, lb: thinner biofilm, ll: lower light intensity and hl: higher light intensity.

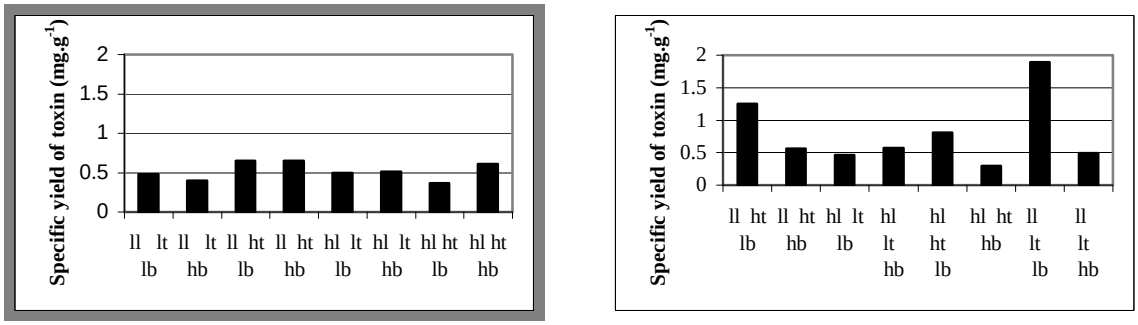

Figure 4.10: Specific yield of toxin for cells exposed to **left)** lower nitrate concentration and **right)** higher nitrate concentration. ht: longer time on membrane. lt: shorter time period on membrane, hb: thicker biofilm, lb: thinner biofilm, ll: lower light intensity and hl: higher light intensity.

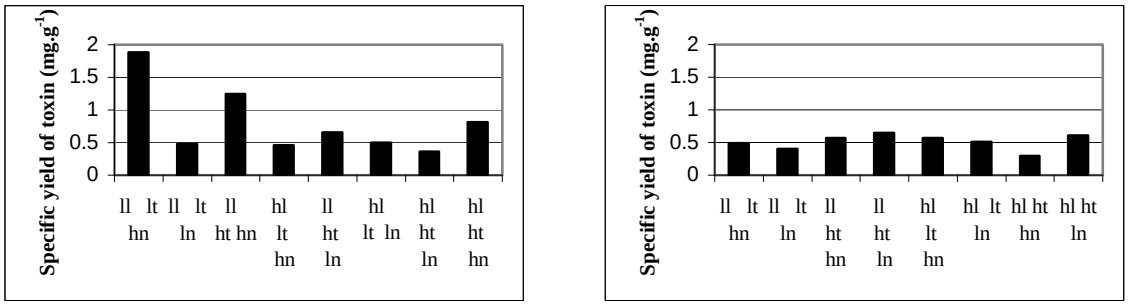

Figure 4.11: Specific yield of toxin for **left)** thinner biofilms and **right)** thicker biofilms. Ht: longer time on membrane, lt: shorter time period on membrane, hn: higher nitrate concentration, ln: lower nitrate concentration, ll: lower light intensity and hl: higher light intensity.

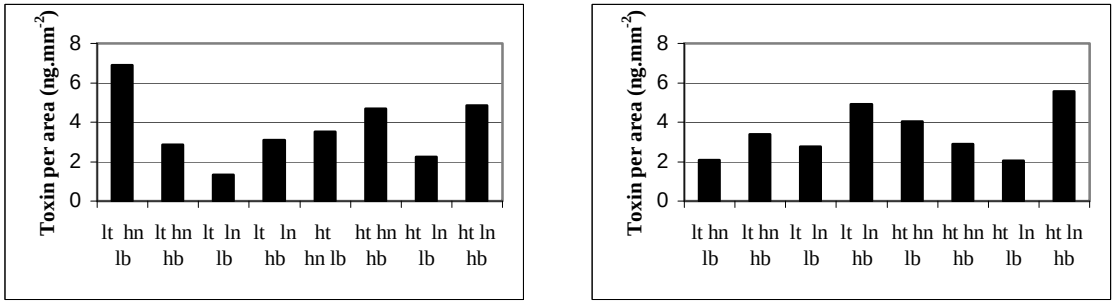

Figure 4.12: Toxin produced (ng) per unit area of membrane (mm^2) for **left)** the lower light intensity and **right)** higher light intensity. ht: longer time on membrane, lt: shorter time period on membrane, hn: higher nitrate concentration, ln: lower nitrate concentration, hb: thicker biofilm, lb: thinner biofilm.

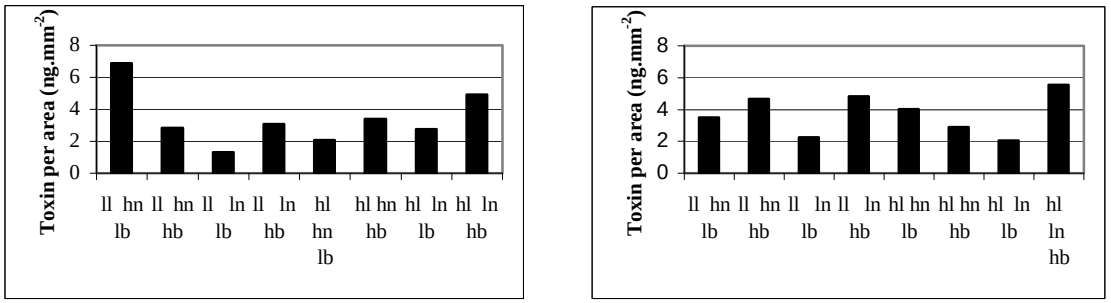

Figure 4.13: Toxin produced (ng) per unit area of membrane (mm^2) for the cells immobilized for **left)** shorter time period and **right)** longer time period. ht: longer time on membrane. hn: higher nitrate concentration, ln: lower nitrate concentration, hb: thicker biofilm, lb: thinner biofilm, ll: lower light intensity and hl: higher light intensity.

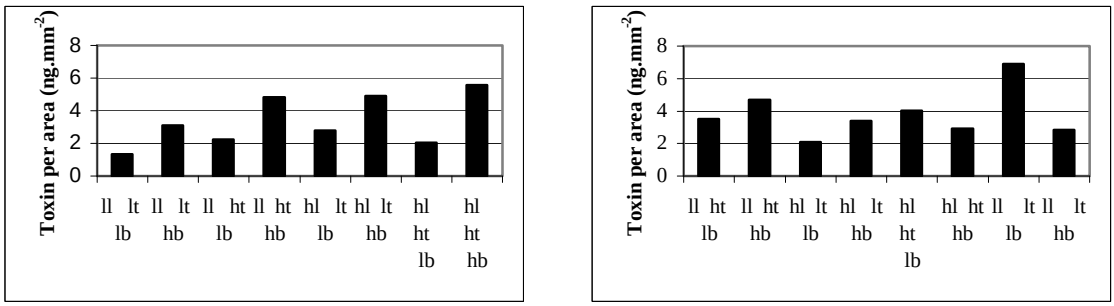

Figure 4.14: Toxin produced (ng) per unit area of membrane (mm^2) for cells exposed to **left)** lower nitrate concentration and **right)** higher nitrate concentration. ht: longer time on membrane. lt: shorter time period on membrane, hb: thicker biofilm, lb: thinner biofilm, ll: lower light intensity and hl: higher light intensity.

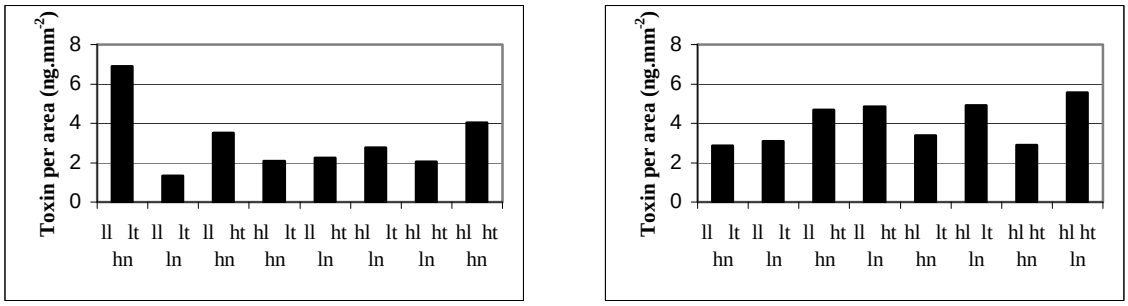

Figure 4.15: Toxin produced (ng) per unit area of membrane (mm^2) for **left)** thinner biofilms and **right)** thicker biofilms. ht: longer time on membrane, lt: shorter time period on membrane, hn: higher nitrate concentration, ln: lower nitrate concentration, ll: lower light intensity and hl: higher light intensity.

The specific yield of toxin was clearly greater for cells exposed to the lower light concentration of 700 lux (Figure 4.8). Other than for one biofilm grown for the shorter time period, majority of the samples grown for the longer time period have a higher specific yield of toxin (Figure 4.9). The cells exposed to the higher nitrate concentration are also predominantly higher in specific toxin yield than the cells exposed to a lower concentration of nitrates (Figure 4.10). From Figure 4.11 it is clear that cells contained in thinner biofilms have a better specific yield of toxin.

The toxin production per area did not show great variance with regards to light intensity or immobilization time period Figure 4.12 and 4.13. The higher nitrate concentration appeared to have a marginally better toxin production per unit area (Figure 4.14). There was a distinct increase in toxin per unit area with increased biofilm thickness, as was to be expected as there were far more cells to produce toxin over a certain area.

When all the data for a particular parameter (e.g. high light intensity or low nitrate concentration) were averaged the same trends were clear even with the variation of four major parameters affecting toxin production and manufacturing inconsistencies present in the membrane. Nitrate concentration, biofilm thickness and light intensity appeared to be the three factors that had the greatest effect on toxin production per cell. Cells exposed to a higher nitrate concentration (20 versus 1 mM) and a lower biofilm thickness (4.2 versus 8.0 $ng.^{-2}$) and a lower light intensity (700 versus 5600 lux) had significantly higher toxin content. There was little difference regarding toxin content of the cells that had been immobilized for five hours and those that had been immobilized for four days. With toxin production per area, biofilm thickness variation was the only parameter to display a notable difference. A thick biofilm, longer time period, lower light intensity and higher nitrate concentration were conducive to an increased production of toxin per mm^2 of membrane.

4.3.5 Induction of secondary metabolite production by complete nutrient deprivation under a high light intensity

The buoyant culture displayed little change in microcystin content over the 18 hour time period (Figure 4.17). These cells were thought to be actively dividing and rich in storage granules. The cells settled within the first two hours of experiment, indicating a physiological response to the high light intensity, by breaking down their gas vesicles. The microcystin content in non-buoyant cells decreased such that by the end of the 18 hours there was no detectable toxin present.

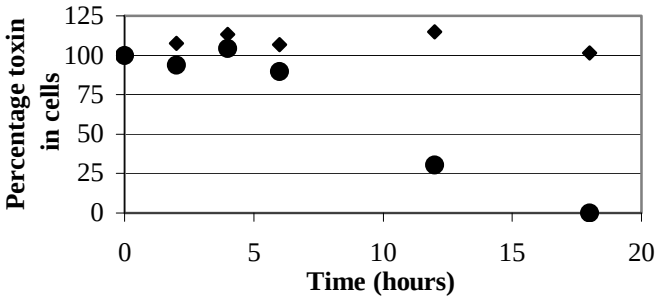

Figure 4.16: Toxin production per cell mass for the two cultures under complete nutrient deprivation and a high light stress shown as a function of time. ●: specific yield of toxin for non-buoyant cells ♦: specific yield of toxin for buoyant cells.

Greatest toxin production with batch cultures occurred when there was a specific amount or ratio of nutrients available to the cells. The data obtained in this experiment suggests that when no nutrients were available to the bacteria they did not produce microcystin, and that there is a minimum nutrient concentration requirement for microcystin production.

4.4 Conclusions

There appeared to be a great variation in toxin production per cell and unit area of membrane with time variation. The primary reason for the variation was that the biofilms were not of equal density. When the data was plotted relative to biofilm density, trends were more evident, indicating that the cells had acclimatized to immobilized conditions fairly rapidly (within 5 hours). Of the parameters tested nitrate concentration, biofilm thickness and light intensity had the greatest effect upon microcystin production under immobilized conditions.

Of the biofilm thicknesses tested thinner ones were more efficient for specific toxin production. The thicker biofilms had a greater yield of microcystin per unit area. The relative

differences in specific toxin production were small in comparison to the differences between production per unit area.

A moderate light intensity of 700 lux had greater microcystin production per cell and unit area than a more intense one of 6000 lux. Cells in their natural environment could decrease their gas vesicle content to escape dangerous light intensities, whereas immobilized bacteria could not.

Higher nitrate concentrations (20 mM) in the nutrient medium resulted in increased microcystin production per cell and unit area. The complete nutrient deprivation and biofilm thickness variation with differing nitrate concentrations established that there was a minimum nitrate requirement for microcystin production. The data obtained suggests that microcystin is produced during conditions that favour growth. When cells are in the stationary growth phase or not metabolically active its concentration decreases. This was not expected since microcystin is generally reported to be produced during stationary phase.

CHAPTER 5
LOCALIZATION OF MICROCYSTIN PRODUCTION BY IMMUNOLABELLING

5.1 Introduction

It was assumed that nutrients diffused from the lumen and were depleted before reaching the outer biofilm, while the light intensity would decrease from the opposite direction as a function of cell density. This led to the hypothesis that microcystin was produced in the biofilm where nutrient and light concentrations were optimal, presumably closer to the base of the biofilm. Immunocytochemistry is a technique for identifying cellular or tissue constituents by means of antibody-antigen interactions, and identifying the site of antibody binding either by direct labeling of the primary antibody, or by use of a secondary labeled antibody (Bancroft and Stevens, 1996). Elucidation of the region of microcystin production was achieved by immunolabelling microcystin-containing cells with a primary antibody to microcystin, linking a secondary antibody conjugated to alkaline phosphatase to the primary antibody, and then using a colorimetric detection system.

With immunocytochemistry optimal ultrastructural preservation is usually obtained using osmium tetroxide in the fixing process, but these fixatives could mask antigenic sites. Strong oxidizing agents had been found to unmask protein antigenic sites on gluteraldehyde-fixed post-osmicated tissues. Oxidizing agents include a saturated alcoholic solution of sodium hydroxide, hydrogen peroxide and periodic acid (Bendayan and Zollinger, 1983; Mar and Wight, 1989).

Although the structure and potency of microcystins had been intensively studied, little was known of their structural localization until Shi *et al*. (1995) used immuno-gold labeling to elucidate where toxins were most prevalent within *M. aeruginosa* PCC7820. A polyclonal antibody to microcystin LR generated in rabbits (method in Chu *et al*., 1989) displayed cross-reactivity to several microcystins. The majority of antibody binding occurred within the thylakoid and nucleoid region, which may have represented the region of synthesis or the region of cellular utilization of the microcystins. Some toxin was found in the cell wall and sheath area, but none in inclusions such as lipid bodies, polyhedral bodies, cyanophycin granules and membrane-limited inclusions. The lack of occurrence near cellular inclusions could indicate that the metabolites were involved in a specific cell activity, and not functioning as a storage compound. Other studies found okadaic acid, also an inhibitor of PP1

and PP2A, only to occur in the chloroplasts of the okadaic acid producing cells. This supported the idea that these metabolites might be related to photosynthetic activities (Shi *et al*., 1995).

The objective of this chapter was to elucidate the location of toxin production within a biofilm immobilized upon a synthetic membrane.

5.2 Methods and materials

5.2.1 Slide preparation

Slides were washed with detergent, rinsed with distilled water, soaked in 95% ethanol for 30 minutes, air-dried, immersed in acetone containing 2% APES (3- amino- propyl- triethoxy-silane) for 10 seconds, air-dried, washed for 5 seconds in pure acetone twice and air-dried.

5.2.2 Sample preparation and immunolabelling

The monoclonal primary antibody to microcystin LR (generated in mice) was purchased from Alexis Corp. It. The secondary antibody was anti-mouse IgG (Fc specific) conjugated to alkaline phosphatase purchased from Sigma. Binding was detected with NBT/BCIP (napthol-AS- phosphate/diazonium salt) from a DIG system kit for filter hybridization from Boehringer Mannheim, which forms a blue precipitate (Bancroft and Stevens, 1996)

Biofilm containing membranes were freeze-dried, set in wax, cut in 8µm thick sections with a microtome, placed on APES-coated slides, coated lightly in xylene and left overnight at 37^{o}C. Wax was removed by immersing slides for 5 minutes in xylene three times. Cells were rehydrated with an ethanol-water series and then blocked in a phosphate buffered saline solution contained Triton X-100 (PBST: PBS at 0.01M phosphate buffer (pH 7.4), 0.3M NaCl, 0.1% sodium azide and 0.1% Triton X-100) with 1% bovine serum albumin (BSA) for half an hour at room temperature. The samples were incubated with the primary antibody (at concentrations of 40, 20, 4, 2, 0.2, 0.4 and 0.004 µg.ml^{-1}) in PBST for 3 hours at room temperature and 24 hours at 4^{o}C. A control sample was incubated with PBST instead of primary antibody. Sections were rinsed three times, using PBST, and blocked for half and hour with PBST containing 0.1% BSA. Samples were incubated with the secondary antibody (1:40 dilution) in PBST at 37^{o}C for half an hour, rinsed three times with PBST and then twice with the buffer used for NBT/BCIP (100 mM Tris-HCl at pH 9.5 containing 100 mM sodium chloride and 50 mM magnesium chloride). The samples were incubated with NBT/BCIP (100

µl of the kit stock solution in 10 ml buffer) for 4 hours in darkness, rinsed three times with distilled water, mounted under a cover slip, viewed with the light microscope and photographed (The method was an adaptation of information from Shi *et al*., 1995, Bancroft and Stevens, 1996, Oncogene research products catalogue, 2001 and Boehringer Mannheim Biochemica DIG system user's guide for filter hybridization, 1993).

5.3 Results and Discussion

The results of the experiment are shown in Figures 5.1 to 5.8. All photographs are displayed such that the lumen is either at the base or left-hand side. The control cells, which were treated with PBST not containing the microcystin antibody and did not yield any distinguishable staining (Figure 5.1a and 5.1b).

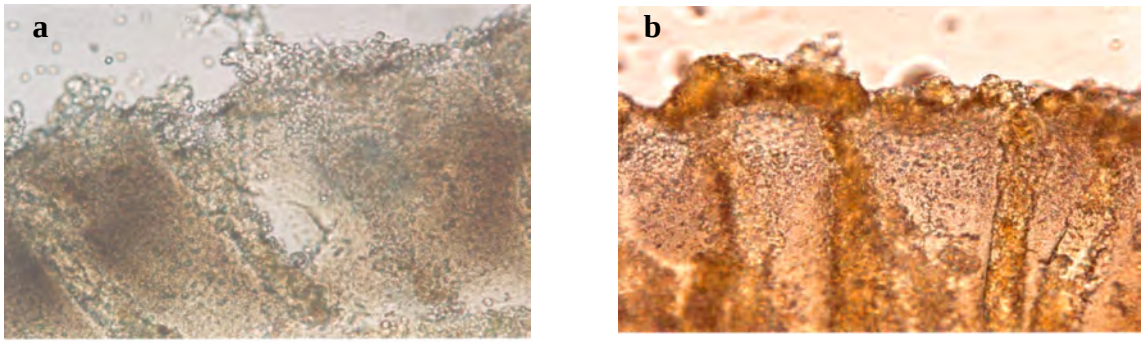

Figure 5.1: Control cells (exposed to PBST with no primary antibody) at a magnification of 256 times.

Staining at the highest primary antibody concentration of 40 µg.ml^{-1} (Figure 5.2a) yielded no visible differences between cells. Cells within the pores and outer biofilm were darkly stained. With lower concentrations, staining became more selective, and it was possible to ascertain where in the biofilm microcystin production was greatest.

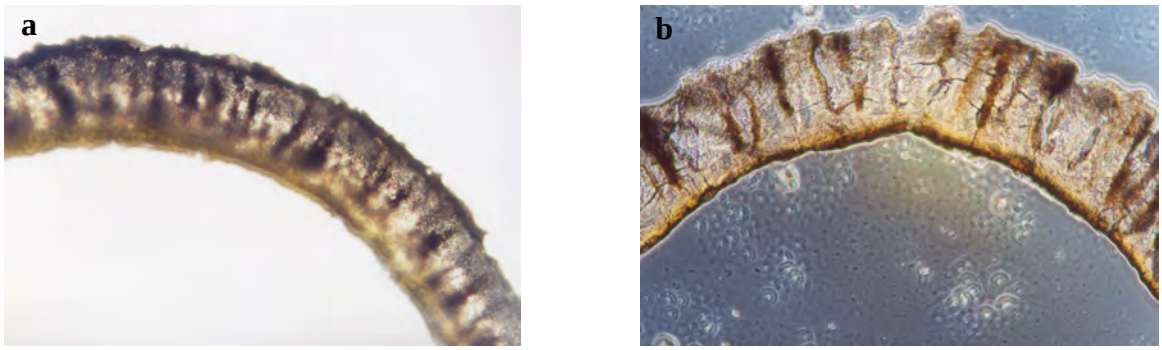

Figure 5.2: Immobilized cells exposed to a primary antibody concentration of **a)** 40 µg.ml^{-1} at a magnification of 100 times and **b)** 20 µg.ml^{-1} at a magnifications of 64 times.

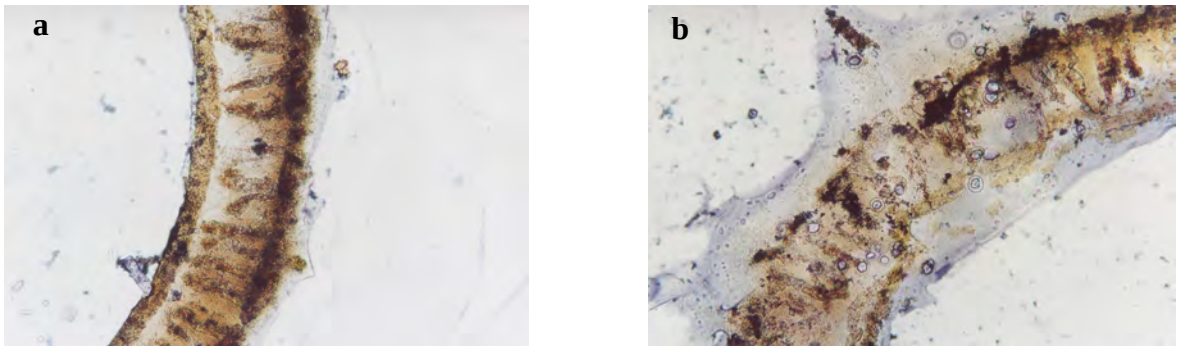

Figure 5.3: Immobilized cells exposed to a primary antibody concentration of 20 µg.ml^{-1} at a magnification of 64 times.

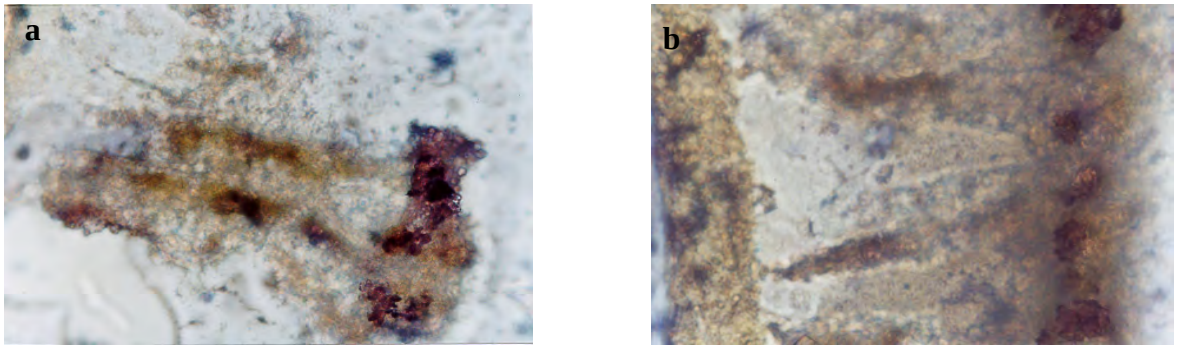

Figure 5.4: Immobilized cells exposed to a primary antibody concentration of **a)** 4 µg.ml^{-1} at a magnification of 284 times and **b)** at a magnification of 256 times.

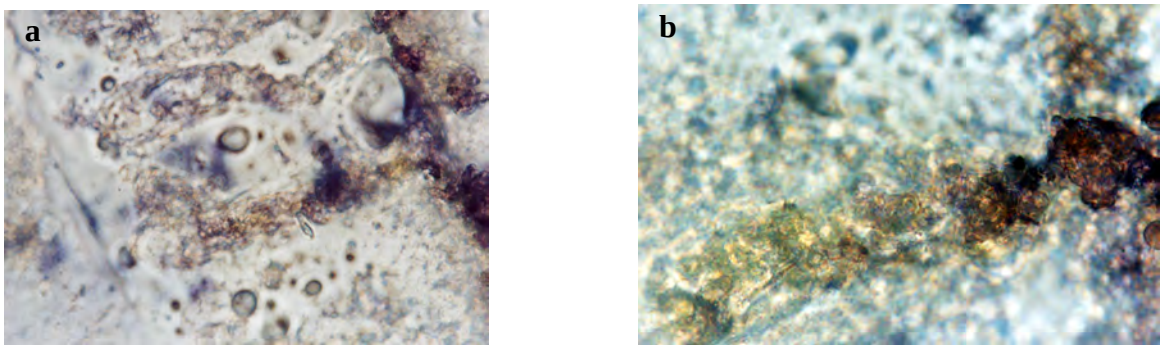

Figure 5.5: Immobilized cells exposed to a primary antibody concentration of **a)** 2 µg.ml^{-1} at a magnification of 256 times and **b)** at a magnification of 418 times.

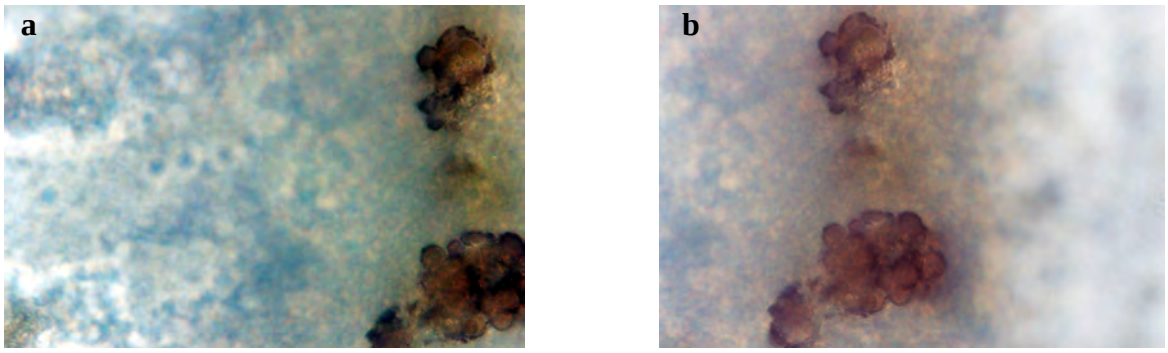

Figure 5.6: Immobilized cells exposed to a primary antibody concentration of **a)** 0.4 µg.ml^{-1} at a magnification of 256 times and **b)** 0.4 µg.ml^{-1} at a magnification of 641 times.

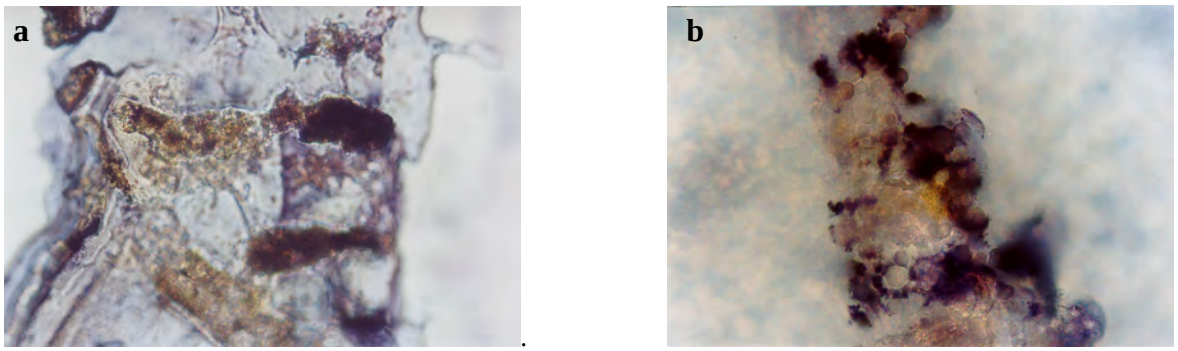

Figure 5.7: Immobilized cells exposed to a primary antibody concentration of **a)** 0.4 µg.ml^{-1} at a magnification of 641 times and **b)** 0.2 µg.ml^{-1} at a magnification of 641 times.

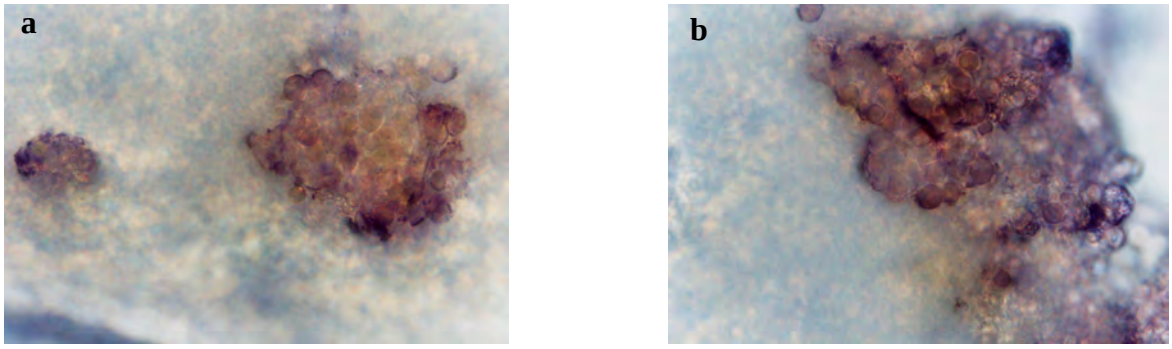

Figure 5.8: Immobilized cells exposed to a primary antibody concentration of **a)** 0.2µg.ml^{-1} and **b)** 0.4 µg.ml^{-1} (both at a magnification of 641 times).

At a primary antibody dilution of 20 µg.ml^{-1} it appeared that toxin production occurred at the base of the biofilm just above the membrane outer surface (Figure 5.2b and 5.3a and 5.7b); presumably where light and nutrients were at concentrations conducive to toxin production. Cells inside the pores receive the greatest amount of nutrients and the least light, and did not have a high microcystin content. Cells outside the pores displayed greater staining, which

corresponded to lower nutrient and higher light concentrations, in accordance to the gradostat concept.

With primary antibody concentrations of 0.2, 0.4, 2 and 4 $\mu g.ml^{-1}$ (Figures 5.4 to 5.5) it was evident that cells in the outer biofilm that contained the greatest quantities of microcystin were not just at the base of the biofilm, but occurred in clusters around the area where the pore opened to the outer membrane surface. Cells were producing toxin in a vein from the pore opening at the membrane surface to the outer biofilm layers (Figures 5.4b and 5.7b), instead of a concentric band extending from the outer membrane base, as was expected. For this to have occurred nutrients were passing from the pore outwards relatively fast, and then diffusing laterally into the biofilm (parallel to the lumen) relatively slower, and not in a gradual gradient from the base. This concept is expanded in Chapter 6. Presumably channels were formed between the cells during immobilization, to allow suspension medium to pass from the extra-capillary space into the lumen. These channels allowed nutrients to diffuse to the outer biofilm layers faster than would have occurred through a solid biofilm. Diffusion of the nutrients would then have occurred sideward in the true gradostat fashion, resulting in a vein of maximal microcystin production in the biofilm above the membrane pore.

At a primary antibody dilution of 0.4 and 0.2 $\mu g.ml^{-1}$ it was seen that even within the veins the microcystin production is greatest at the point of contact with the external membrane pore surface. Figures 5.6b and 5.8a all showed a cluster of cells, above the pores but below the outer biofilm surface, producing microcystin. This was also visible at a primary antibody dilution of 2 $\mu g.ml^{-1}$ in Figure 5.6a.

Microcystin was produced in a dome shape just above the pore when there was enough distance between them not to allow for a nutrient overlap (Figure 5.8b). The gradostat concept was not adhered to completely due to a) distance between the pores and b) the channels formed in the biofilm during immobilization. Cells situated in outer biofim layers were receiving more nutrients than cells situated between pore spaces at the outer membrane surface.

5.4 Conclusion

An immunocytochemical method was successfully developed to visualise microcystin production in the cyanobacterial biofilm with sufficient resolution. This, together with the

membrane system, offers a powerful tool to study the impact of nutrient and light gradients on toxin production in cyanobacterial biofilms. This could generate new insights into what triggers toxin production in algal blooms, since the membrane system more closely resembles the natural environment of these organisms than conventional flask culture.

CHAPTER 6
FINAL DISCUSSION AND CONCLUSIONS

A variety of membranes and modules were used for the immobilization of *Microcystis aeruginosa* PCC7806. The best immobilization occurred on the externally skinless polyethersulfone membranes. The externally skinless polyethersulfone membranes were inexpensive and versatile. The disadvantage of this membrane was its melting point of 55^{o}C, which resulted in a longer sterilization process using 4% formaldehyde and then flushing with water. The membrane was also inconsistent with regards to pore distribution and thickness of internal skin as well as formation of an external skin.

Bacterial adhesion to the membranes was dependent on the physiology of the cell culture. Cells in the stationary phase, which had a well-developed EPS layer and no gas vesicles, were optimal for immobilization. This was a problem in that cells had to pass through the stage at which optimal toxin production occurred for batch cultures before they could be immobilized. This would have been less of a problem if the cells were more productive once immobilized, and if the toxin could have been extracted in a continuous manner.

Results reflected that a thin biofilm, under a moderate light intensity with a high nitrate concentration in the growth medium in the lumen allowed for the most efficient toxin production per biomass. A thick biofilm, under a moderate light intensity with a high nitrate concentration in the growth medium in the lumen allowed for best toxin production per unit area.

Overall microcystin yield was much lower for immobilized cells than that of batch culture. The production under immobilized conditions had a yield of 0.5 to 1.5 mg toxin per gram of dry cell mass. This was far less efficient than batch culture where 5 to 8 mg toxin was produced per gram dry mass.

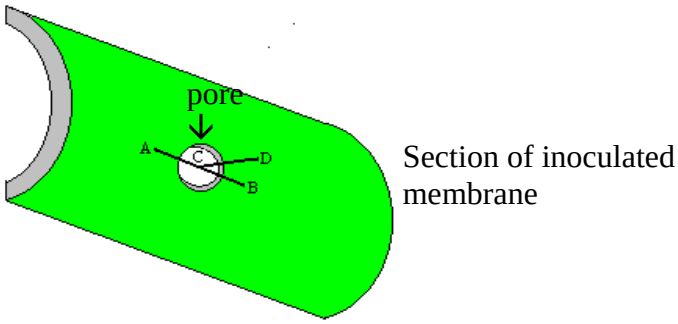

Figure 6.1: Schematic of a membrane section illustrating the regions across a pore from a to b and c to d from which the profiles of nutrient concentration, stage of growth and microcystin production are derived that are shown in Figures 6.2, 6.3 and 6.4.

Immunolabelling revealed cells around the base of the biofilm, where the cells were outside the pores, had the highest microcystin content. The nutrient gradient was more prevalent parallel to the lumen than perpendicular to it. Veins of microcystin containing cells were prominent in the biofilm above the pores. Microcystin production occurred in a cluster at this point, as nutrients diffused into the cells to the sides of the vein. Figures 6.2 and 6.3 illustrate an explanation for this manner of toxin production. The cross section of the area represented in Figure 6.3 and 6.4 is shown in the diagram in Figure 6.1.

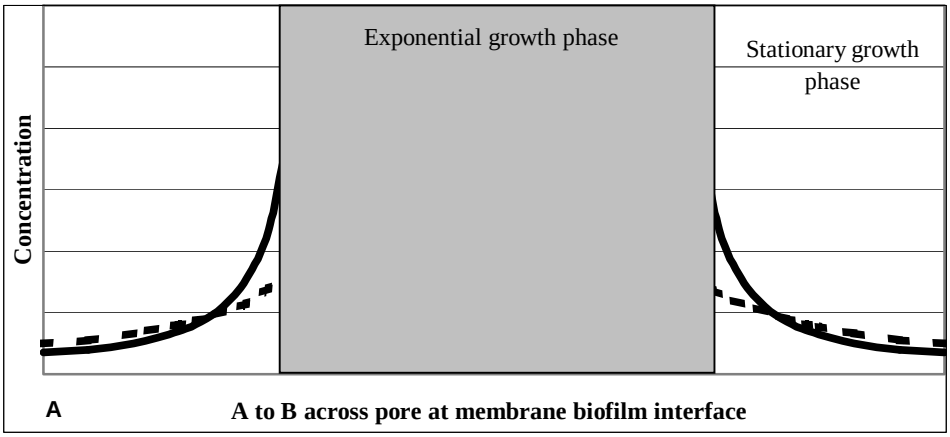

Figure 6.2: Explanation of nutrient gradient, growth stage and toxin production across the biofilm at the outer membrane across a pore (A to B in Figure 6.1). ---- = microcystin production – = nutrient concentrations

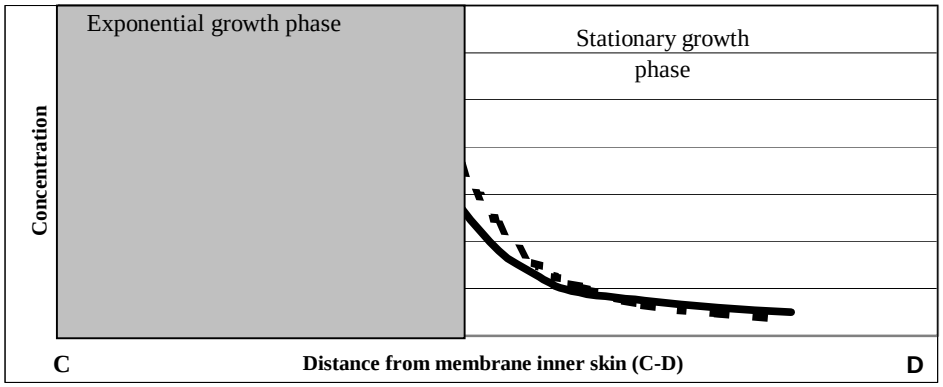

Figure 6.3: Explanation of nutrient gradient, growth stage and toxin production from within a pore to the outer biofilm surface (C to D in Figure 6.1). ---- = microcystin production **–** = nutrient concentrations

For *Microcystis aeruginosa* PCC7806, immobilized in biofilms thicknesses from 3-12 $ng.mm^{-2}$, by pressure inoculation, the nutrient gradostat concept needed to be modified to the fact that sideward movement of the nutrients from the veins produced a greater gradient than movement toward the outer layers of the biofilm. Production was only notable in cells out of the pores, where the light intensity was high enough to induce toxin production. Channels formed during immobilization were allowing nutrients to diffuse outwards in a manner quicker than anticipated, which led to these clusters of microcystin production.

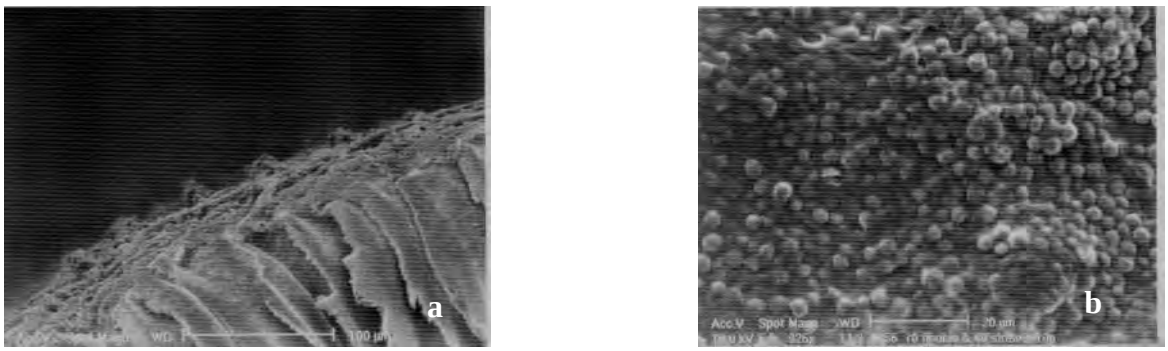

Figure 6.3: Scanning electron micrographs of **a)** mounds of cells visible on the biofilm surface (magnification of 365 times) and **b)** the irregular outer biofilm surface (magnification of 925 times).

Distinct mounds of growth were seen in Figure 6.3a, while Figure 6.3b showed an undulating outer biofilm surface, indicating that growth was also occurring in mounds around the pores. These biofilms were cultured for two weeks with a BG-11 medium in the lumen that had a 20 mM nitrate concentration, and prepared for SEM as described in Chapter 2. These mounds were a result of cell division in the immediate region of the pore, and were a clear indication that growth was also affected by the pore dispersion on the membrane. The mounds were a result of cell division at and directly around the pore.

Microcystin is a metabolite that appears to be involved in primary growth, but its production peaks just prior to the onset of stationary growth, as a secondary metabolite would. This meant that cells in the outer biofilm that were nutrient stressed, such that they are in the stationary growth phase, produced very little microcystin. This is a novel finding that contradicts currently published theories. Thus it can be concluded that the membrane bioreactor could become a very useful tool in understanding toxin production in cyanobacterial biofilms. In terms of the development of the membrane photobioreactor for the production of microcystins, considerable work still needs to be done to optimise production yield to make it a competitive system.

REFERENCES

Ash C., Mackintosh C., Mackintosh R. and Fricker C.R. 1995. Development of a colorimetric protein phoshorylation assay for detecting cyanobacterial toxins. *Water Science and Technology* **31:**47-49.

Bancroft J.D. and Stevens A. 1996. Theory and practice of histological techniques fourth edition. pp 437 and 394. Churchill Livingstone, Hong Kong.

Barbosa H.R. and Alterthum F. 1992. The role of extracellular polysaccharide in cell viability and nitrogenase activity of *Beijerincka derxii*. *Canadian Journal of Microbiology* **38:**986-988.

Bendayan M. and Zollinger M. 1983. Ultrastructural localization of antigenic sites on osmium-fixed tissues applying the protein A-gold technique. *Journal of Histochemistry and Cytochemistry* **31:**101-109.

Berner T. 1993. Ultrastructure of the microalgae, CRC Press, USA, pp22-24

Blackburn S.I., McCausland M.A., Bolch C.J.S., Newman S.J. and Jones G.J. 1996. Effect of salinity on growth and toxin production in cultures of the bloom-forming cyanobacterium *Nodularia spumigena* from Australian waters. *Phycologia* **35:**511-522.

Brown M.J. and Lester J.N. Aug 1980. Comparison of bacterial extra-cellular polymer extraction methods. *Applied and Environmental Microbiology* **40:**179-185.

Burton S.G., Boshoff A., Edwards W., Jacobs E.P., Leukes W.D., Rose P.D., Russell A.K., Russell I.M. and Ryan D. 1998. Membrane based biotechnological systems for the treatment of organic pollutants. WRC Report No 687/1/98.

Chetsumon A., Maeda I., Umeda F., Yagi K., Miura Y. and Mizoguchi T. 1994. Antibiotic production by the immobilized cyanobacterium *Scytonema* TISTR 8208, in a seaweed–type photobioreactor. *Journal of applied Phycology* **l6:**539-543.

Choi H.J., Tao B.Y. and Okos M.R. 1995. Enhancement of secondary metabolite production by immobilized *Gossypium arboreum* cells. *Biotechnological Progress* **11:**306-311.

Chu F.S., Huang X., Wei R.D. and Carmichael W.W. 1989 Production and characterization of antibodies against microcystins. *Applied and Environmental Microbiology* **55:**1928-1933.

Chung B.H. and Chang H.N. 1998. Aerobic fungal cell immobilization in a dual hollow fibre bioreactor: continuous production of citric acid. *Biotechnology and Bioengineering* **32:**205-211.

De Maagd P.G., Hendriks A.J., Seinen W. and Sijm D.T.H.M. 1999. pH hydrophobicity of the cyanobacteria toxin microcystin LR *Water Research* **33:**677-680.

Falconer I.R. 1993. Algal toxins in seafood and drinking water. pp145-205 Academic Press Harcourt Brace & Company, London.

Fastner J. Flieger I. and Neumann U. 1998. Optimized extraction of microcystins from field samples – a comparison of different solvents and procedures. *Water Research* vol **32:**3177-3181.

Frazier K., Colvin B., Styer E., Hullinger G. and Garcia R. 1998. Microcystin toxicosis in cattle due to overgrowth of blue-green algae. *Veterinary Human Toxicology* **40:**23-24.

Gathercole P.S. and Thiel P.G. 1987. Liquid chromatographic determination of the cyanoginosins, toxins produced by the bacterium *Microcystis aeruginosa*. *Journal of chromatography* **408:** 434-438.

Gorham P.R. 1964. Toxic algae. pp307-336 In: Algae and man. Ed Jackson D.F. Plenum Press, New York.

Jensen T.E. 1985. Cell inclusions in the cyanobacteria. *Archives of Hydrology* Suppl 71 ½ Algological Studies 38/39 p33-75.

Kaebernick M., Neilan B.A., Borner T. and Dittmann E. 2000. Light and the transcriptional response of the microcystin biosynthesis gene cluster. *Applied and Environmental Microbiology* **66:**3387-3392

Lee S.J., Jang M.H., Kim H.S., Yoon B.D and Oh H.M. 2000. Variation of microcystin content of *Microcystis aeruginosa* relative to medium N:P ratio and growth stage. *Journal of Applied Microbiology* **89:**323-329

Mar H. and Wight T.N. 1989. Correlative light and electron microscopic immunocytochemistry on reembedded resin sections with colloidal gold. in: Colloidal gold: principles, methods and applications volume two. pp361-362 edited by Hayat M.A. Academic Press, San Diego.

Markov S.A., Lichtl R., Kao K.K. and Hall D.O. 1993. A hollow fiber photobioreactor for continuous production of hydrogen by immobilized cyanobacteria under partial vacuum. *International Journal of Hydrogen Energy* **18:**901-906.

Markov S.A., Bazin M.J. and Hall D.O. 1995. Hydrogen photoproduction and carbon dioxide uptake by immobilized *Anabaena variabilis* in a hollow fiber bioreactor. *Enzyme and Microbial Technology* **17:**306-310.

Neilan B.A., Dittmann E., Rouhiainen L., Bass R.A., Schaub V., Sivonen K. and Borner T. 1999. Non ribosomal peptide synthesis and toxigenicity of cyanobacteria. *Journal of Bacteriology* **181:**4089-4097.

Oh H., Lee S.J., Jang M. and Yoon B. 2000. Microcystin production by *Microcystis aeruginosa* in a phosphorous limited chemostat. *Applied and Environmental Microbiology* **66:**176-179.

Oncogene Research Products Catalog 2001. Apoptosis third edition. p418 CN Biosciences an affiliation of Merck.

Prescott L.M., Harley J.P. and Klein D.A. 1996. Microbiology third edition. pp459-465 Wm.C Brown Publishing Co., New York.

Rae B. Moollan R.W. and Clark R.C. 1999. Algal toxins in drinking water supplies. WRC Report No 549/1/99

Rapala J., Sivonen K., Lyra C., and Niemela S. 1997. Variation of microcystins, cyanobacterial hepatotoxins, in *Anabaena spp*. as a function of growth stimuli. *Applied and Environmental Microbiology* **63:**2206-2212.

Romans K.M., Carpenter E.J. and Bergman B. 1994. Buoyancy regulation in the colonial diazotrophic cyanobacterium *Trichodesmium tenue*: ultrastructure and storage of carbohydrate, polyphosphate and nitrogen. *Journal of Phycology* **30:**935-942.

Schluchter W. and Glazer A.N. 1999. Biosynthesis of phycobilliproteins in cyanobacteria. in: The phototrophic prokaryotes edited by Peschek G.A., Loffelhardt W. and Schmetterer G. pp83-96 Kluwer Academic/Plenum Publishers, New York.

Shi L., Carmichael W.W. and Miller I. 1995. Immuno-gold localization of hepatotxins in cyanobacterial cells. *Archives of Microbiology* **163:**7-15.

Skulberg O.M., Codd G.A. and Carmichael W.W. 1984. Toxic blue-green algal blooms in Europe: a growing environmental problem. *Ambio* **13:**244-247.

Utkilen H. and Gjolme N. 1992. Toxin production by *Microcystis aeruginosa* as a function of light in continuous cultures and its ecological significance. *Applied and Environmental Microbiology* **58:**1321-1325.

Utkilen H. and Gjolme N. 1995. Iron-Stimulated toxin production in *Microcystis aeruginosa*. *Applied and Environmental Microbiology* **61:** 797-800.

van der Westhuizen A.J. and Eloff J.N. 1985. Effect of temperature and light on the toxicity and growth of the blue-green algae *Microcystis aeruginosa* (UV-006). *Planta* **163:**55-59.

Walsby A.E., Beard S.J. and Hayes P.K. 1999. The natural selection of gas vesicles. in: The phototrophic prokaryotes edited by Peschek G.A., Loffelhardt W. and Schmetterer G. pp633-646. Kluwer Academic/Plenum Publishers, New York.

Ward C.J., Beattie K.J., Lee E.Y.C. and Codd G.A. 1997. Colorimetric phosphatase inhibition assay of laboratory strains and natural blooms of cyanobacteria: comparisons with high performance liquid chromatographic analysis for microcystins. *FEMS Microbiology Letters* **153:**465-473.

Watanabe M.F. and Oishi S. 1985. Effects of environmental factors on toxicity of a cyanobacterium (*Microcystis aeruginosa*) under culture conditions. *Applied and Environmental Microbiology* **49:**1342-1344.

Watanabe M.F., Harada K., Matsuura K., Watanabe M. and Suzuki M. 1989. Heptapeptide toxin production during the batch culture of two *Microcystis* species (Cyanobacteria). Journal of Applied Phycology **1**:161-165.

White D. 2000. The physiology and biochemistry of the prokaryotes 2nd edition. pp27, 28, 133, 145-148 and 311. Oxford University Press.

Wicks R.J. and Thiel P.G. 1990. Environmental factors affecting the production of peptide toxins in floating scums of the cyanobacterium *Microcystis aeruginosa* in a hypertrophic African reservoir. *Environmental Science and Technology* **24:**1413.

Wiedner C., Visser P. and Mur L.R. 2001. Effects of light on microcystin content on *Microcystis aeruginosa* PCC2805 studied in continuous cultures under steady state, transient state and on a diurnal time scale. Fifth international conference on toxic cyanobacteria manual, Noosa, Queensland Australia.

Yoshizawa S., Matsushima R., Watanabe M.F., Harada K., Ichihara A. Carmichael W.W. and Fujiki H. 1990. Inhibition of protein phosphatases by microcystis and nodularian associated with hepatotoxicity. *Cancer Research and Cliinical Oncology* **116:**609-614.

Websites

WS1) http://www.brain-tec.de/mutants.htm

WS2) http://www.che.bham.ac.uk/research_labs/gani/noular.html

WS3) http://www.nal.usda.gov/bic/Biotech_Patents/1995patents/05413928.html

APPENDIX

BG 11 growth medium

Table A.1: Microelement stock solution (made up to 1000 ml)

H_3BO_3	2.680g
$MnCl_2.4H_20$	1.810g
$Na_2MoO_4.2H_20$	0.391g
$ZnSO_4.7H_20$	0.222g
$CuSO_4.5H_20$	0.079g
$Co(NO_3)_2.6H_20$	0.049g

Table A.2: BG-11 solution (made up to 1000ml)

EDTA	0.003 g
$FeCl_3.6H_20$	0.003 g
$NaNO_3$	1.590 g
K_2HPO_4	0.039 g
$MgSO_4.7H_20$	0.075 g
Na_2CO_3	0.020 g
$Ca(NO_3)_2.4H_20$	0.020 g
$Na_2SiO_3.5H_20$	0.043 g
Citric acid	0.006 g
Microelement stock solution	1 ml

The final pH is adjusted to 7.8 with 1M HCL or 1M NaOH. (Rae *et al*., 1999)

For Table A.1 to A.13 biofilm thickness is represented as the cell dry mass (ng) divided by the biofilm-covered surface area expressed (mm^2), toxin production per cell is represented by total toxin produced (μg) divided by the dry mass of the cells (mg) and toxin production per unit area is expressed as total toxin produced (ng) divided by the biofilm-covered surface area of the membrane (mm^2).

Table A.3: Results for biofilms sacrificed over a thirty day period.

Sample day	Biofilm thickness (ng/ mm^2)	Specific yield of toxin (mg/g)	Toxin production per unit area (ng/ mm^2)
0		5.7	
3	12.1	6	72.6
6	8.8	5.1	44.8
9	9.9	6.2	61.3
12	9.5	5	47.7
15	8.1	9.3	75.8
18	8.8	8.9	78.2
21	10.7	7.4	79.2
24	10.1	31.6	318.3
27	10.5	8.6	90.0
30	10.7	9.1	97.0

Table A.4: Results for biofilms sacrificed over a 7-day period.

Day	Biofilm thickness (ng/ mm^2)	Specific yield of toxin (mg/g)	Toxin production per area (ng/ mm^2)
Control		0.597	
1	3.92	0.941	3.69
2	3.32	0.935	3.10
3	5.34	0.476	2.54
4	6.58	0.653	4.30
5	3.12	0.754	2.35
6	4.1	0.447	1.83
7	4.94	0.389	1.92

Table A.5: Results for various biofilm thicknesses grown for 10 days with two nitrate concentrations under a moderate (700 lux) light intensity.

No.	Nitrate concentration	Biofilm thickness (ng/ mm^2)	Specific yield of toxin (mg/g)	Toxin production per area (ng/ mm^2)
1	20 mM	2.78	0.243	0.7
2	20 mM	4.62	0.68	3.1
3	20 mM	5.4	1.127	6.1
4	20 mM	5.7	0.805	4.6
5	20 mM	6.74	1.045	7
7	20 mM	8.78	0.757	6.6
8	20 mM	9.68	1.042	10.1
9	1 mM	2.42	0.539	1.3
10	1 mM	3.46	0.376	1.3
11	1 mM	5.1	0.108	0.5
12	1 mM	6.18	0.364	2.2
13	1 mM	6.8	0.203	1.4
14	1 mM	8.28	0.173	1.4

Table A.6: Results of toxin production for two cell cultures under complete nutrient deprivation

Time	Specific yield of toxin for buoyant cells (mg/g)	Specific yield of toxin for non-buoyant cells (mg/g)
0	0.204	0.115
2 hours	0.219	0.108
4 hours	0.231	0.120
6 hours	0.218	0.103
12 hours	0.234	0.035
18 hours	0.207	0.000